Ore Geology Reviews 85 (2017) 247–270

Contents lists available at ScienceDirect

Ore Geology Reviews

journal homepage: www.elsevier.com/locate/oregeorev

Listvenite-related gold deposits of the South Urals (Russia): A review

Elena V. Belogub [a,b,*], Irina Yu. Melekestseva [a], Konstantin A. Novoselov [a], Mariya V. Zabotina [a], Gennady A. Tret'yakov [a], Victor V. Zaykov [a], Anatoly M. Yuminov [b]

[a] Institute of Mineralogy, Urals Branch of Russian Academy of Sciences, 456317 Miass, Chelyabinsk District, Russia
[b] South Urals State University, Miass Branch, 8 Iyulya St. 10, Miass, Chelyabinsk District 456301, Russia

ARTICLE INFO

Article history:
Received 9 September 2015
Received in revised form 31 October 2016
Accepted 11 November 2016
Available online 24 November 2016

Keywords:
Orogenic gold
South Urals
Oxygen isotopes
Listvenite
Fluid inclusions

ABSTRACT

The Urals is a complex fold belt, which underwent long geological evolution. The formation of most gold deposits in the Urals is related to the collision stage. In this paper, we review some relatively small listvenite-related gold deposits, which are confined to the large Main Uralian fault zone and some smaller faults within the Magnitogorsk zone. The Mechnikovskoe, Altyn-Tash, and Ganeevskoe deposits are studied in detail in this contribution. They comprise the ore clusters along with other numerous small gold deposits, and constituted the sources for the gold placers exploited in historical time. The gold is hosted by metasomatites (listvenites, beresites) and quartz veins with economic gold grades (up to 20 g/t Au). Listvenites are developed after serpentinites and composed of quartz, fuchsite, and carbonates (magnesite, dolomite) ± albite. Volcanic and volcanoclastic rocks are altered to beresites, consisting of sericite, carbonates (dolomite, ankerite), quartz and albite. Pyrite and chalcopyrite are major ore minerals associated with gold; pyrrhotite, Ni sulfides, galena, sphalerite, arsenopyrite and Au-Ag tellurides are subordinate and rare. Gold in these deposits is mostly high-fineness (>900‰). The lower fineness (~800‰) is typical of gold in assemblage with polymetallic sulfides and tellurides. The ores have been formed from the NaCl–CO_2–H_2O ± CH_4 fluids of low (~2 wt% NaCl-equiv.) to moderate (8–16 wt% NaCl-equiv.) salinity at temperatures of 210–330 °C. The oxygen isotopic composition of quartz ($\delta^{18}O$) varies from 14.7 to 15.4‰ (Mechnikovskoe deposit), 13.2 to 13.6‰ (Altyn-Tash deposit) and 12.0 to 12.7‰ (Ganeevskoe deposit). The oxygen isotopic composition of albite from altered rocks of the Ganeevskoe deposit is 10.1‰. The calculated $\delta^{18}O_{H2O}$ values of the fluid in equilibrium with quartz are in a range of 5.7–6.3, 4.2–4.6 and 6.3–6.7‰ respectively, and most likely indicate a magmatic fluid source.

1. Introduction

Gold mining in the Urals started in the second half of the 18th century and it is still active (Sazonov et al., 1999). The earliest record on gold production goes as early as the Bronze Age (Zaykov et al., 2012). More than 1000 t of gold have been extracted in the Urals during 250 years of mining, half of which was mined in the South Urals. Extraction of placer gold brought a well-deserved honor to the South Urals gold-bearing province. At present, gold in the South Urals is mostly a by-product of massive sulfide deposits mining. However, relatively large Bereznyakovskoe, Kochkar and Svetlinskoe gold deposits in Chelyabinsk district are also being mined. The South Urals resource base also includes numerous small sub-economic lode gold deposits, which were the major sources for gold placers. Some of them are associated with specific metasomatic rocks (listvenites).

In the Russian scientific literature dedicated to Urals, most attention was traditionally paid to the large gold deposits (Sazonov et al., 1999; Kisters et al., 1999; Kolb et al., 2000; Bortnikov, 2006), and deposits with atypical geological setting or debatable genesis (Murzin et al., 2001, 2002; Spiridonov and Pletnev, 2002; Murzin and Shanina, 2007; Znamensky and Michurin, 2013; Plotinskaya et al., 2009). Numerous small deposits, which are located within the Main Uralian fault (MUF) zone and smaller regional faults, were mostly studied in the first half of the 20th century (see review in Znamensky, 2009) and later on were almost completely ignored by researchers, although listvenite occurrences with gold deposits are traced along the entire MUF zone. The results of their previous studies of this specific deposit type are scattered in unpublished exploration reports and briefly summarized in the Russian publications (Sazonov et al., 1999; Znamensky, 2009).

* Corresponding author at: Institute of Mineralogy, Urals Branch of Russian Academy of Sciences, 456317 Miass, Chelyabinsk District, Russia.
E-mail address: belogub@mineralogy.ru (E.V. Belogub).

http://dx.doi.org/10.1016/j.oregeorev.2016.11.008
0169-1368/

Listvenites and associated quartz–sericite–carbonate metasomatites (beresites) are the alteration products of ultramafic and mafic (in less extent, intermediate to felsic) rocks, respectively. The process of alteration occurs under influence of CO_2- and S-rich fluids (Sazonov, 1998; Zharikov et al., 2007). Listvenites are mainly composed of quartz, carbonates (dolomite and magnesite), sericite (fuchsite or mariposite) and pyrite (Fig. 1a–e). The other alteration assemblage is made up of quartz, carbonates of dolomite–ankerite series, sericite, albite and pyrite (Fig. 1f).

The term "listvenite" was proposed by Gustav Rose in 1837 for the green rocks from the lode gold deposits of the Miass ore region. Its root is based on the Russian name for a larch tree (Rose, 1837). The term "beresite" was described for the first time at the Berezovskoe gold deposit in the Central Urals and its name derives from the deposit's name. Previously, the terms "listvenite" and "beresite" were used mostly in Russian geological literature (e.g., Kashkay and Allakhverdiev, 1965; Sazonov, 1998; Obolensky and Borisenko, 1978). Over the last years, these terms became also common in English geological literature, but "beresite" occurs rarely and its definition is contradictory (Ash and Arksey, 1990; Zharikov and Zaraisky, 1991; Halls and Zhao, 1995; Botros, 2004; Baksheev and Kudryavtseva, 2004; Yaghubpur and Abedi, 2005; Yigit, 2006; Zoheir and Lehmann, 2011). Nevertheless, these terms were recommended for usage by the IUGS Subcommission on the Systematics of Metamorphic Rocks (Zharikov et al., 2007).

Gold in these metasomatic rocks occurs as inclusions in pyrite (refractory gold), metasomatites or selvage of carbonate–quartz veinlets and veins (Fig. 1d). Gold-bearing quartz, quartz–carbonate or quartz–albite veins are typical constituents of listvenites (Fig. 1b–d).

It is commonly accepted that granitic magmatism is responsible for the formation of most productive listvenite-related gold deposits (Buisson and Leblanc, 1986; Sazonov, 1998; Likhoidov et al., 2007). However, some deposits are not spatially associated with granitic plutons or their size is rather small. For example, the Au-bearing listvenites in the Iranian metaophiolites are regarded as a result of metamorphic dehydration and decarbonation reactions of the oceanic crust at the amphibolite–greenschist facies (Aftabi and Zarrinkoub, 2013).

The lode gold deposits in listvenites are known in the suture zones of Russia, Iran, Turkey, Egypt, Morocco, Ireland, Canada and other countries (e.g., Buisson and Leblanc, 1986; Aydal, 1990; Halls and Zhao, 1995). The largest deposits are situated in the Barramiya–Um–Salatit ophyolite belt in Egypt, where they have been exploited for a few thousand years since the Pharaoh Period. The El Barramia and some other deposits are of economic interest (Zoheir and Lehmann, 2011). Several large listvenite-related gold deposits with ore reserves of 1–2 Mt and Au grades of 3–5 g/t are known in the Atlin ore district, Canada (Ash and Arksey, 1990; Hansen et al., 2005). In Russia, gold deposits in listvenites are mostly small. For example, the resources of the Khaak-Sair deposit in West Sayany (Siberia) are ~18 t (mean of 2 g/t with a range from 0.5 to 57 g/t Au) (Kuzhuget et al., 2015).

In this paper, we review the small subeconomic listvenite-related gold deposits of the South Urals. The interest in these deposits is twofold: first, they constitute the sources of gold for the rich gold placers, and, second, their features reflect the metallogenic potential of large tectonic zones. The ore bodies at these deposits are mostly localized in collision structures (Sazonov et al., 1999; Znamensky, 2009). Granitic intrusions within the deposits are either unknown or rather small. These features are also typical of other deposits mentioned in the paper, allowing us to consider them as orogenic-style deposits (cf., Groves et al., 1998). Taking into account their importance for the resource base of the South Urals and ambiguous genesis, the aim of our work is to review the mineral composition of ores and metasomatites, and to establish the formation conditions and fluid sources for these deposits. These features may be specific to the processes related with the late subduction and/or early collision stages (Puchkov, 2016; Herrington et al., 2005; Kisters et al., 1999). The specific features of these deposits are then compared with large deposits, the origin of which is related to the gabbro–tonalite–granodiorite–granitic magmatism of the Main Plutonic Axis of the Urals (cf., Fershtater et al., 2007, 2010; Fershtater, 2013).

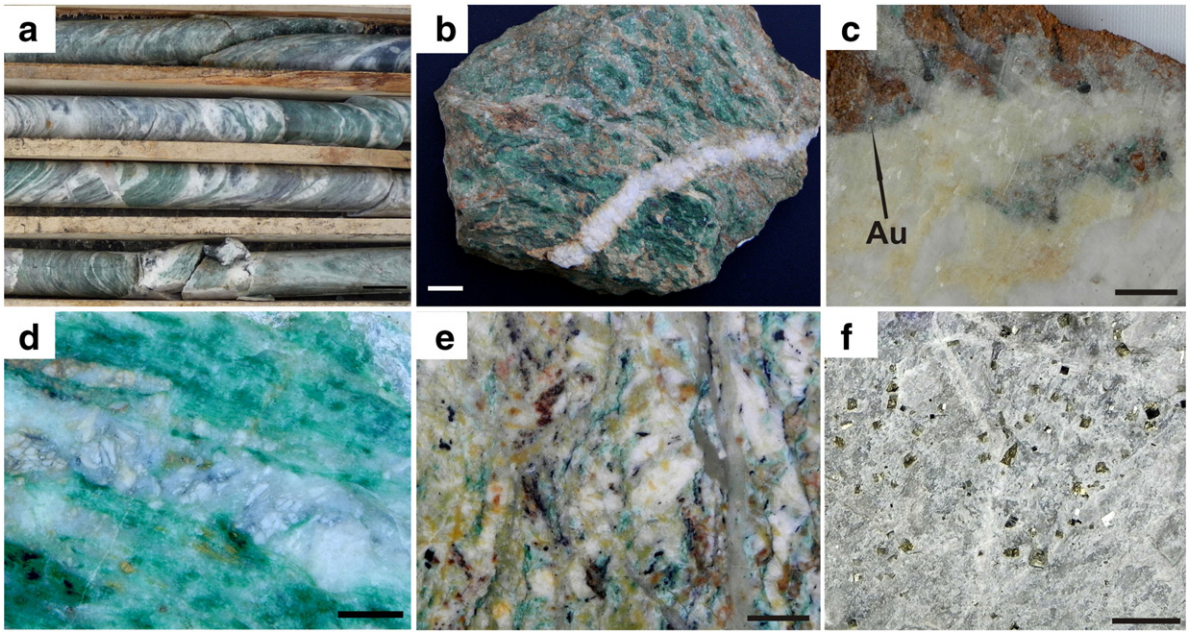

Fig. 1. Gold-bearing listvenites and beresites from the South Urals deposits: a – alternation of schistose listvenites and beresites with quartz veins; b – listvenite with zonal carbonate–quartz vein; c – free gold in oxidized listvenite near calcite–quartz vein; d – listvenite with quartz–albite vein; e – albite-bearing listvenite with quartz vein; f – beresite. Scale bar: a – 5 cm, b–f – 1 cm. Photos: a – Altyn-Tash deposit, b, d – Miass ore field; c – Mechnikovskoe deposit; e, f – Ganeevskoe deposit.

2. Distribution of gold deposits in the South Urals

Six longitudinal zones can be distinguished within the structure of the southern part of the Urals fold belt: Pre-Uralian foredeep (PUF), West Uralian (WUZ), Central Uralian (CUZ), Magnitogorsk (MZ), East Uralian (EUZ) and trans-Uralian (TUZ) (Fig. 2a) (Puchkov, 1997, 2016; Herrington et al., 2005). The PUF, WUZ and CUZ represent the passive margin of the East European platform (EEP), which was formed in the Late Cambrian to Early Ordovician, evolved in Ordovician, Silurian and Devonian, and was finally deformed in Carboniferous to Permian to become a part of the Urals fold belt (Puchkov, 2016). The MZ complexes are compared with the rocks of the oceanic basins (ophiolites), island arcs, Andes-type belts, flischoid troughs and inter-arc basins. They are divided from the complexes of the EEP passive margin by the MUF, which is one of the largest suture zones of Eurasia (Fig. 2b). It was originated in the Early Paleozoic and was repeatedly renewed in the Late Paleozoic and Mesozoic (Puchkov, 1997, 2016; Herrington et al., 2005). Major gold deposits of the South Urals are confined to the MUF, MZ and EUZ. Some gold deposits are known in TUZ. The WUZ and PUF host no significant gold deposits.

Economic gold deposits of the South Urals are distinct in size, composition of ores, Au grades, geological structure and genesis. According to the composition of ores and technological requirements, the lode gold deposits can be classified as gold–quartz and gold–sulfide. The gold–quartz type includes low-sulfide deposits, which are mostly of orogenic type. The listvenite-related deposits reviewed in our paper also belong to this type. The gold–sulfide type includes a broad genetic spectrum of the deposits with the higher amount of sulfides in ores, which are either hosted by the volcano-sedimentary rocks and belong to porphyry–epithermal systems, or related to the volcanic-hosted massive sulfide (VHMS) deposits (Fig. 2). No listvenites are typical for these types of the deposits.

The MUF hosts numerous small vein and stringer–disseminated gold deposits, the formation of which is related to the brittle deformations during early collision (Puchkov, 2016; Znamensky, 2009). The listvenite-related gold deposits are traced almost throughout the entire MUF and they also are typical of some large faults of the MZ. In our work, we describe gold deposits of the North Miass, Miass, Altyn-Tash, Karan–Alexandrovsky and Mindyak ore fields of the MUF (Fig. 2). In contrast to these deposits, the most famous Zolotaya Gora gold deposit is associated with serpentinized harzburgites of the MUF zone and controlled by bodies of the garnet–diopside–chlorite rodingites, which replace the mafic dikes (Sazonov et al., 1999; Kisters et al., 1999; Spiridonov et al., 1997).

The MZ island arc complexes are host to the numerous VHMS deposits, with gold as a major by-product, along with some small Au-bearing VHMS occurrences (e.g., Kontrol'NOE) (Servakin et al., 1994). The MZ also hosts economic gold deposits with disseminated polymetallic sulfides in volcano-sedimentary rocks (e.g., West Kurosan and Murtykty) (Fig. 2). The West Kurosan deposit is characterized by some features typical of epithermal-style deposits (Plotinskaya et al., 2016 and reference therein) and was formed synchronously with the Devonian volcanism.

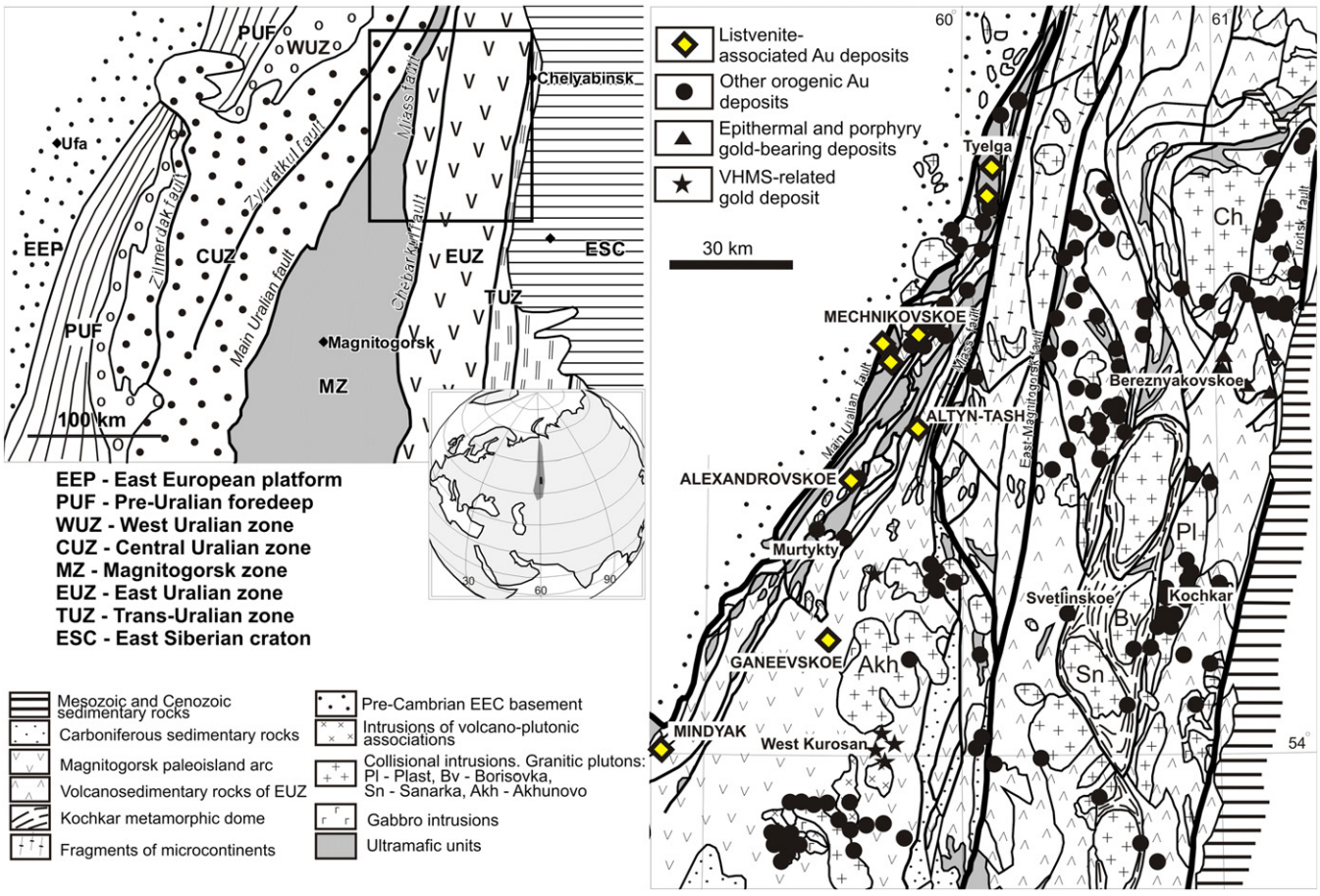

Fig. 2. Geodynamic setting of lode gold deposits of the South Urals, modified after Geological map of Russian Federation on a scale of 1:1 000 000, N-40(4) (edited by V.I. Kozlov), 2001, Herrington et al. (2005) and Puchkov (2016).

The Murtykty deposit, which is situated near the MUF, is considered to be formed during collision processes responsible for silicification and carbonatization of primary gold-bearing volcanic rocks (Sazonov et al., 1999). Numerous small gold–quartz deposits within the MZ are confined either to the contacts of the large collisional granites plutons (Fig. 2), or to the regional fault zones. For example, the Ganeevskoe deposit occurs within the Karagayly regional fault zone, and can be ascribed to the orogenic type.

The EUZ is divided from the MZ by the East Magnitogorsk fault and is characterized by a complex block structure, which includes the fragments of microcontinents, oceanic and island arc complexes and tonalite–granodiorite–granitic and granite–adamellitic intrusions of different age, which belong to the Main Granitic Axis of the Urals. Here, the deeper crustal levels have been exhumed into the surface during collision. Some of these collision-related granitic plutons are combined with surrounding metavolcanic and sedimentary rocks into the Kochkar metamorphic dome. The country rocks of this block underwent metamorphism up to amphibolite facies. Such a complex structure results in combination of different gold and gold-bearing deposits.

The gold-bearing porphyry copper (e.g., Tomino) and epithermal (e.g., Bereznyakovskoe) deposits are hosted by the island arc complexes (Plotinskaya et al., 2009). The veined and stringer–disseminated gold–quartz type includes the Kochkar and Svetlinskoe deposits. The first one has more than 300 t of gold production over the last 170 years. The latter has more than 100 t of reserves. Both of them are ascribed to the collisional gabbro–tonalite–granodiorite–granitic magmatism in the Kochkar metamorphic block (Kisters et al., 1999; Kolb et al., 2000; Fershtater et al., 2010; Puchkov, 2016).

The TUZ is composed of a system of the parallel longitudinal anticlines and synclines combined along the faults. The Riphean and Paleozoic blocks in this zone are mostly overlapped by the Mezosoic–Cenozoic sedimentary cover. The iron skarn deposits are the major mineral deposits of the TUZ. Only some gold-bearing porphyry copper (e.g., Mikheevka) and related Au–Cu skarn deposits (e.g., Varvarinskoe) are known here (Puchkov, 2016; Plotinskaya et al., 2016). Some orogenic gold deposits of this zone are located in Kazakhstan (e.g., Dhzetygara).

3. Sampling and methods

3.1. Sampling

The samples for this study were collected in several field campaigns: 1) in 2010–2012, from the open pit of the Ganeevskoe deposit; 2) in 2011–2013, from old mines of the Mechnikovskoe and Altyn-Tash deposits, and (3) in 2012, from the drill core of the Altyn-Tash deposit. The description of other listvenite-related deposits is based on the published data (Sazonov et al., 1999; Murzin et al., 2001, 2002, 2007; Znamensky and Michurin, 2013) and unpublished reports.

3.2. Mineral chemistry

Samples were studied by transmitted and reflected light microscopy using Axiolab CZ, Axioscope A.1 and Olympus BX51 microscopes at the Institute of Mineralogy, Miass, Russia (IMin UB RAS). Bulk mineralogical composition was confirmed by X-ray diffractometry using Shimadzu XRD-6000 diffractometer (Cu*K*-alpha radiation with a monochromator). The quantitative estimation was conducted using constant coefficients method at the IMin UB RAS. The chemical composition of minerals was analyzed using a REMMA-202 M and Vega3 Tescan scanning electron microscopes at the IMin UB RAS. First one is equipped with a Link ED-System operating at 1 μm electron beam, 15 nA beam current, 20 kV accelerating voltage, counting time of 120 s. The latter SEM is equipped with an EDA X-Act Oxford instruments and operates at 3 μm electron beam, 20 nA beam current and 20 kV accelerating voltage, with counting time of 120 s. The standards used for this study are the MINM-25-53 from ASTIMEX Scientific Limited (mineral mount No. 01-044) and a registered standard No. 1362 (Microanalysis Consultants Ltd.). The contents of major oxides were determined at IMin UB RAS by titration (Al_2O_3 (>5 wt%), MgO (>5 wt%), FeO, CO_2), gravimetric analysis (SiO_2, H_2O^-, LOI), colorimetry (Al_2O_3 (<5 wt%), TiO_2, Fe_2O_3, P_2O_5), and atomic absorption (MnO, MgO, CaO, Na_2O, K_2O).

3.3. Fluid inclusion studies

The estimation of ore formation conditions was based on the fluid inclusion study. Primary fluid inclusions (cf., Roedder, 1984) in gold-bearing quartz from the Mechnikovskoe, Altyn-Tash and Ganeevskoe deposits were studied in double-polished thin sections. The temperatures of homogenization (T_h and T_{hCO2}), eutectic (T_e), final ice melting (T_m), and CO_2 melting (T_{mCO2}), were measured using a THMSG-600 (LINKAM) equipment at the South-Urals State University, Miass Branch, Russia. The salt composition of the fluids was estimated from the eutectic temperatures after Borisenko (1977). The salinities of the fluids were calculated from the temperatures of final ice melting following Bodnar and Vityk (1994). The pressure was estimated following Simonov (1981) on the basis of temperature of partial (T_{CO2}) and (T_h) full homogenization of three-phase aqueous–carbonic inclusions. The temperature of partial homogenization allows estimation of the density of the CO_2, which, in assemblage with temperature of full homogenization, can be used to assess the pressure. T_{mCO2} (see below) indicates that the vapor phase is dominated by CO_2, thus we can neglect the presence of other gases, the small amount of which cannot significantly affect the estimated values.

3.4. Oxygen isotopes

Oxygen isotopic composition was determined in quartz from gold-bearing veins in listvenites of the Mechnikovskoe, Altyn-Tash, and Ganeevskoe deposits. Within the Ganeevskoe deposit, the oxygen isotopes were also measured in: (a) quartz from veins in beresites, (b) late galena- and telluride-bearing veins, and (c) listvenites, and (d) rock-forming albite from beresites. The analysis was carried out at the Analytical Center of the Far East Geological Institute, Far East Branch, Russian Academy of Sciences (Vladivostok, Russia).

The samples 1–2 mg in weight were prepared for the analysis using a MIR-10-30 (New Wave Research, United States) infrared continuous laser. BrF_5 was used for oxygen extraction. The released oxygen was further cleaned on the cryogenic traps, absorbent and MOLSIV capillary column. The oxygen isotopic composition was measured on a Finnigan MAT 253 mass spectrometer (Thermo Scientific, Germany) using a double injection system. The results were calibrated on the basis of the NBS-28 and UWG-2 standards (Valley et al., 1995). Reproducibility of $\delta^{18}O$ (1σ) measurements was 0.1‰. Oxygen isotopic compositions of quartz are reported as $\delta^{18}O$ per mil relative to the international standard VSMOW. The $\delta^{18}O_{H2O}$ values of the fluid in equilibrium with quartz were calculated on the basis of quartz–water fractionation equation of Clayton et al. (1972).

4. Geology of the deposits

The southern part of the MUF hosts several ore fields with gold deposits from north to south: North Miass (Tyelga deposit), Miass (Mechnikovskoe deposit), Altyn-Tash (Altyn-Tash deposit), Karan–Alexandrovsky (Alexandrovskoe deposit) and Mindyak (Mindyak deposit) (Fig. 2). The Buyda ore field with Ganeevskoe deposit is located within the Karagayly fault zone of the MZ.

4.1. North Miass ore field, Tyelga deposit

The North Miass ore field is extended for 15 km to the north from the town of Miass. The ore field includes more than ten small gold deposits, which were mined in the 19th–20th centuries and yielded about 1 t of gold. All the deposits are associated with small gabbro–diorite intrusions and located at the contact zone of serpentinites and volcanosedimentary complex of basalt and basaltic andesite composition (Sazonov et al., 1999).

The Tyelga deposit (60.14516° N, 55.31752° E), a typical deposit of this area (Fig. 3), is known from the first half of the 19th century. The deposit has been mined to depth of 40–65 m. Two gold nuggets of 14.37 and 9.5 kg in weight were found in the southern part of the deposit (Sazonov et al., 1999). The ore bodies are composed of quartz (±albite) veins and stockwork zones up to 7 m thick, which are mainly hosted by diorites and, partly, serpentinites (in the southern part of the deposit). The almost vertical gold–quartz veins are concordant with the structural fabric of the host rocks. Listvenites and beresites are developed after serpentinites and diorites, respectively. Gold is unevenly distributed in quartz veins. Pyrite is the major ore mineral; chalcopyrite, galena, fahlore and Bi-, Ag- and Au-tellurides are rare. Two types of gold are revealed on the basis of its mineral assemblage and chemical composition: (i) the low-fineness (901–911‰) gold, which occurs as very small (few micrometers) inclusions in pyrite, and (ii) the high-fineness (913–950‰) coarser (up to 1–2 μm in size) gold, associated with gangue minerals. The temperature (~395 °C) and pressure (~0.7 kbar) of ore formation were established by Sazonov et al. (1999) using calcite-dolomite geothermometer.

4.2. Miass ore field, Mechnikovskoe deposit

The Miass ore field is mostly known as a placer area, where a gold rush started in the beginning of the 19th century. In 1842, a unique gold nugget "*Big triangle*" 36.2 kg in weight was found in the Tashkutarganka River, within the area of the Mechnikovskoe deposit. About 29 t of gold was extracted from placers in the basin of this river. This part of the gold-bearing region was named a "gold bottom". In addition to the Mechnikovskoe deposit, there are many small lode gold deposits, which have periodically been mined by individual miners for more than 200 years (Fig. 4).

4.2.1. Geological outline of the deposit

The deposit is located 21 km southwest of town of Miass (59.86177° N, 54.90291° E) (Fig. 4). It was discovered by mining engineer E. I. Mechnikov in 1797 and has periodically been mined to depths of 30–40 m by small quarries and mines (Borodaevsky, 1948). From 1797 to 1929, about 3270 kg of gold had been extracted here (unpublished report of Kuraev et al., 1939). The deposit is confined to the MUF structure and localized at the NNE–SSW contact of two sheets made up of ultramafic rocks in the east and volcanic rocks in the west (Fig. 5). The contact between these sheets is thought to be tectonic with a strike of 15–25° N and a dip of 75–85°, which correspond to the general direction of the MUF. Small dioritic pluton is located 3 km north-northwest from the deposit (Fig. 4).

The ultramafic sheet is composed of antigorite serpentinites and their altered varieties including listvenites, whereas volcanic sheet consists of diabases, porphyry basalts, metasomatic rocks after volcanic rocks including beresites, volcanoclastic rocks and black shales (Melekestseva et al., 2011).

Antigorite serpentinites host lenses of listvenites and carbonate–talc rocks (Fig. 5). They are accompanied by talc–carbonate alteration along the contact with volcanic rocks. These rocks are also host to the NE- and N-trending blocks of light gray cherts up to 20 m long and up to 4.5 m thick and are cut through by numerous NE-trending dikes a few meters thick of chloritized basalts and altered spessartites. The chemical composition of serpentinites is shown in Table 1. Serpentinites contain relics of chromite.

The lower part of the volcanic sheet represented by *metadiabases* has a direct contact with serpentinites (Fig. 5). By chemical composition, metadiabases are similar to basalts of the Early to Middle Devonian Irendyk Formation (Table 1) (cf., Frolova and Burykova, 1977). The upper part of the volcanic sheet is composed of *porphyritic metabasalts* (Fig. 5), the structure and chemical composition of which are similar to trachibasalts (Table 1).

The volcanic sequence is overlapped by a horizon of strongly foliated carbonatized and chloritized volcanomictic *metasandstones, metagravelstones,* and *metabreccias* of the Middle Devonian Karamalytash Formation with interlayers of clayey shales (Fig. 5). The sedimentary section is crowned by chloritized, epidotized and carbonatized *aphyric* to *slightly porphyritic metabasalts* of the Karamalytash Formation (unpublished report of Chernoostrovets et al., 1999) (Fig. 5).

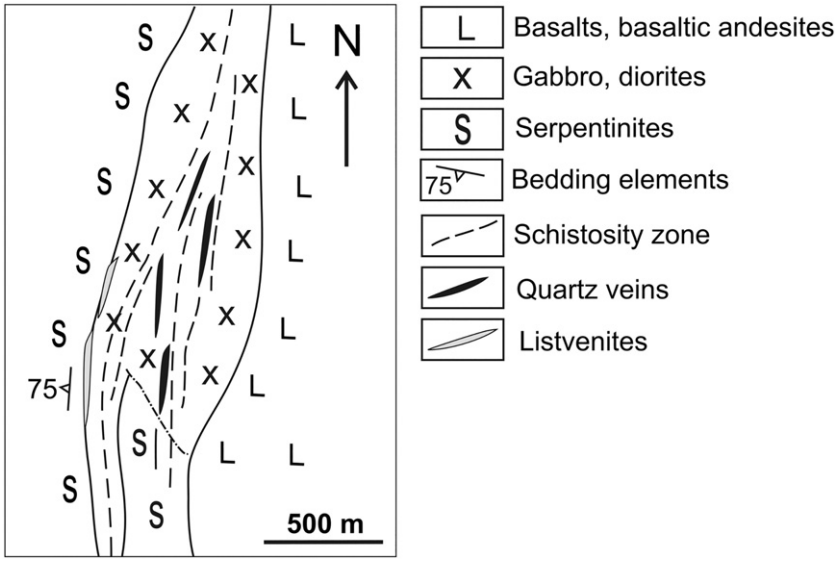

Fig. 3. Geological structure of the Tyelga deposit after Sazonov et al. (1999).

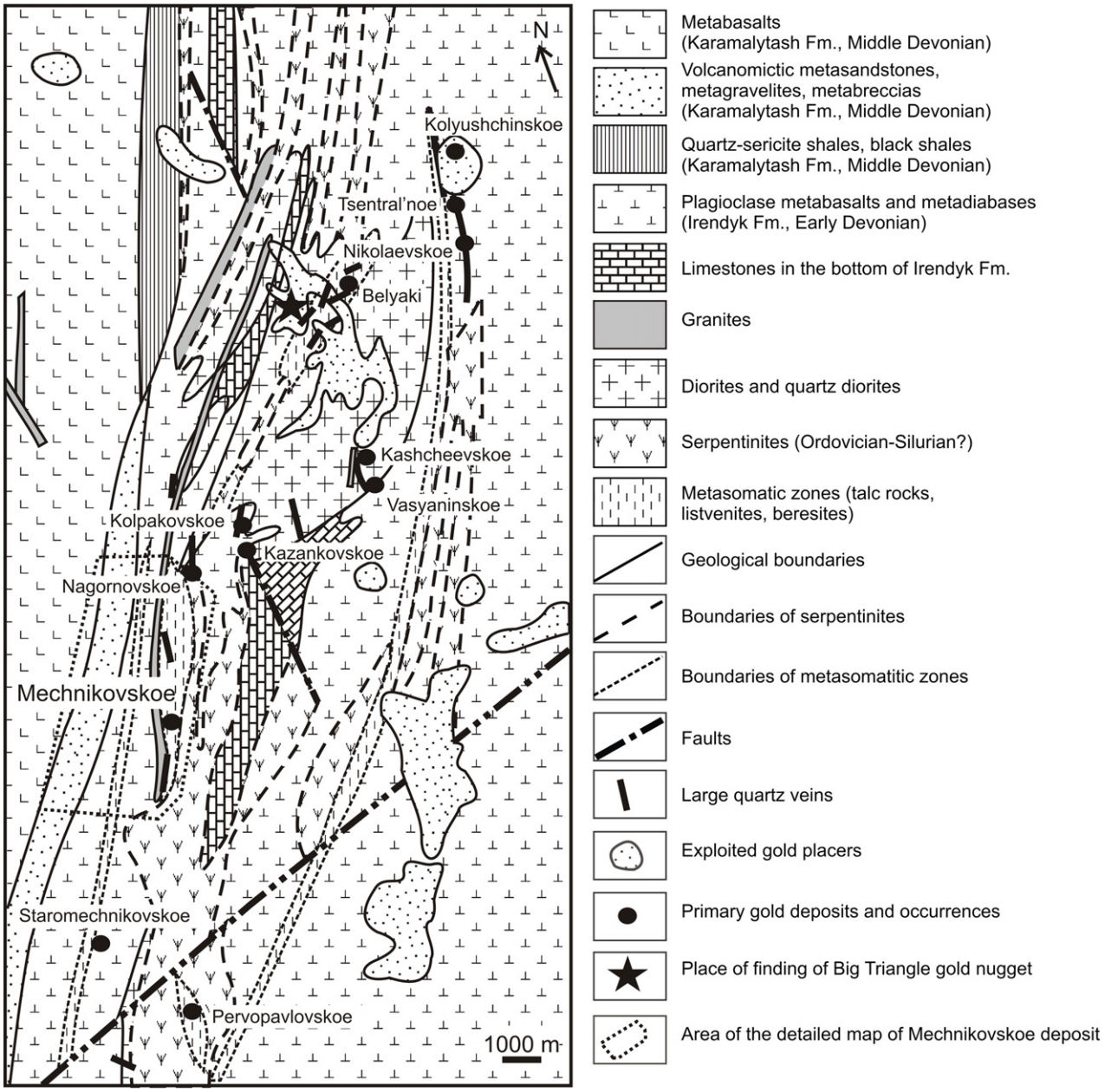

Fig. 4. Geological structure of a fragment of the Main Urals fault zone in the area of the Mechnikovskoe deposit, simplified and modified after unpublished report of Chernoostrovets et al. (1999).

The volcanic sheet is cut by a small-grained granitic dike up to 30 m thick, which occurs almost parallel to the contact of the tectonic sheets. Granites are strongly altered and composed of quartz, sericite, albite and dolomite with relict primary quartz, plagioclase and orthoclase. They contain numerous pyrite crystals up to 1 mm in size. Strong alteration is reflected in chemical composition of the rocks (Table 1).

The ore zone with the ore bodies (Au-bearing listvenites and beresites) is confined to the tectonic contact and, in the central part of the deposit, has contact with granitic dike.

Listvenites form scattered 1.5–10 m-thick echelon-like lenses in ultramafic sheet, which are extended along the strike for ~1 km and traced along the dip to 72 m (Borodaevsky, 1948) (Fig. 5). The maximum Au grade of listvenites is 2.5 g/t (unpublished report of Borodaevsky and Borodaevskaya, 1946). Listvenites are composed of variable amounts of quartz, carbonates (magnesite, dolomite and rare calcite), fuchsite (Cr-bearing mica) and pyrite and are characterized by banded and, locally, schistose structure. The rocks are cut through by quartz and carbonate–quartz veins up to 15 cm thick, which contain sulfides and gold mostly in selvages (Fig. 1c). Listvenites contain relics of chromite, which is replaced by magnetite and fuchsite from the rims. The Cr_2O_3 content in fuchsite varies from 2–3 to 8–10 wt% in aggregates replacing the rock matrix and chromite, respectively. *Talc-carbonate rocks* are composed of magnesite (rarely, dolomite) and talc, and contain subordinate to rare pyrite and arsenopyrite.

Beresites form a body up to 450 long and 50–150 m thick, which is traced to depth of 34 m, and occur at the contact of volcanic rocks and granitic dike (Fig. 5). They are developed after both metadiabases and porphyry metabasalts, and locally retain the relict textures of primary rocks. Beresites are made up of quartz, sericite and albite, as well as subordinate dolomite, epidote, chlorite and actinolite. The SiO_2 content of beresites supports their formation after mafic rocks (Table 1). Albite, along with quartz and carbonate, also forms veinlets up to 1 cm thick.

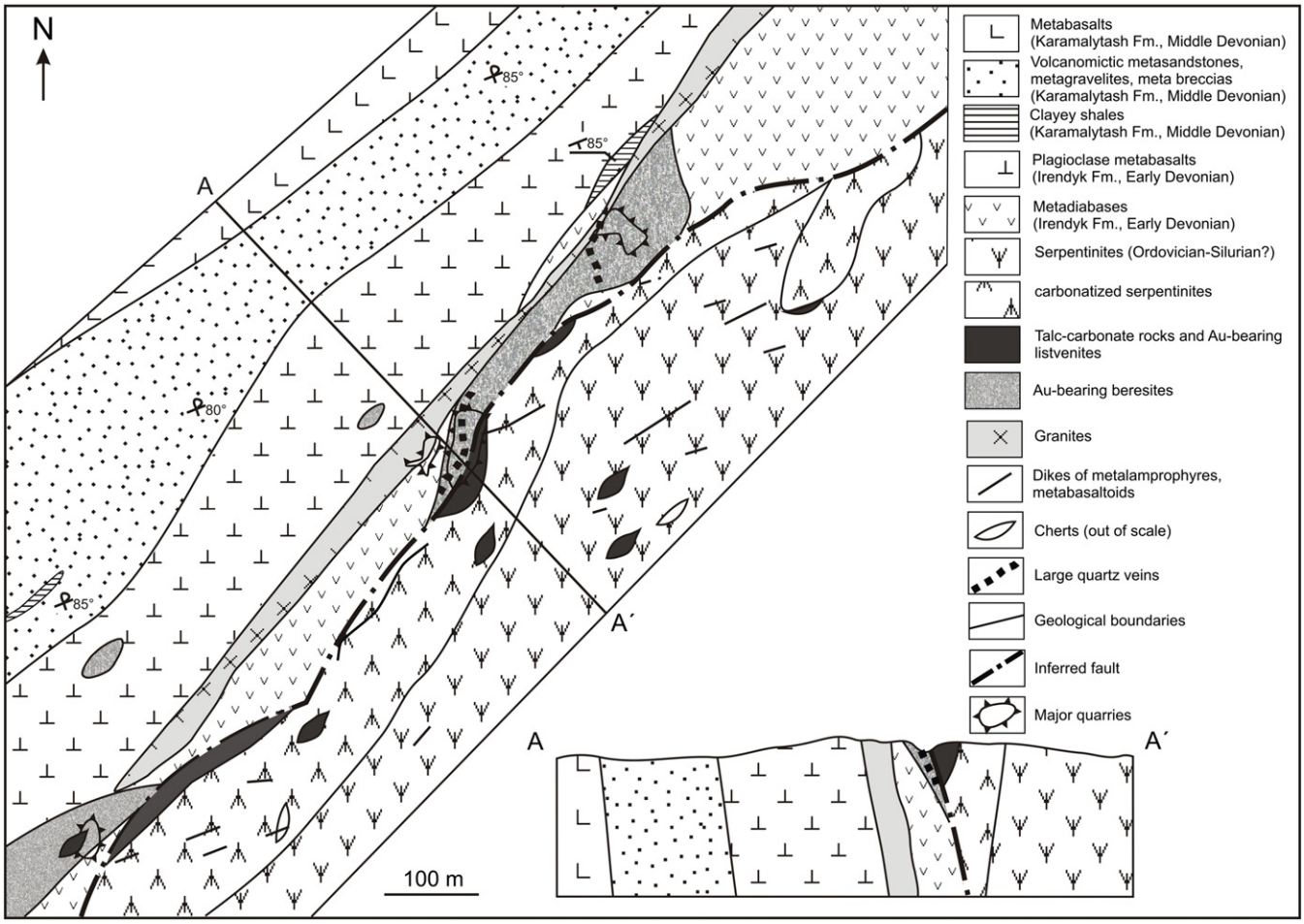

Fig. 5. Geological structure of the Mechnikovskoe deposit, composed by I.Yu. Melekestseva and G.A. Tret'yakov.

Beresites contain numerous pyrite crystals up to 1 mm in size with inclusions of native gold. According to unpublished data of Kvokov et al. (1944), the Au grade of beresites attains 20 g/t in the upper horizons and decreases to 2 g/t with depth. In the central and northern parts of the deposit, beresites host large quartz veins up to 1.5 m thick and up to 120 m long, which contain 1.2–5.9 g/t Au.

Black shales, the samples of which were collected from the dump in the northern part of the largest quarry, are also part of the structure of the deposit, although no outcrops of these rocks were found (Fig. 5). The rocks are cut through by carbonate–quartz veinlets ~1.5 mm thick with small albite crystals in selvages. Pyrite crystals up to 1 mm in size contain inclusions of gold.

4.2.2. Ore mineralogy

Pyrite is a major ore mineral of the deposit; rutile, magnetite and hematite are also abundant. Accessory and rare minerals include chalcopyrite, galena, pyrrhotite, sphalerite, nickeline, fahlores, melonite, cubanite, nickeline, chromite, native gold, Au- and Ag-tellurides, goethite, secondary copper sulfides and iodargyrite.

Pyrite in listvenites and beresites occurs as disseminated cubic metacrystals and their aggregates from several micrometers to 1–3 mm in size. It is also abundant in black shales and quartz veins. Pyrite is host to inclusions of chalcopyrite, pyrrhotite, galena, fahlores, gold (Fig. 6a–d), petzite (Fig. 6e, f), carbonates, sericite and quartz. In listvenites, pyrite with inclusions of gold, petzite and galena contains up to 6.8 wt% Ni and up to 3.5 wt% Co.

Chalcopyrite and *fahlores* occur as large anhedral inclusions, subhedral crystals or intergrowths from a few micrometers to 100 μm in size in the coarse-crystalline pyrite and rock matrix. Fahlores include tennantite (0.6–2.1 wt% Sb, up to 0.2 wt% Ag) and Ag-bearing tetrahedrite (3.2–7.2 wt% As, 0.2–0.3 wt% Ag). *Cubanite* is intergrown with small (~10 μm) pyrite crystals. *Galena, pyrrhotite* and *sphalerite* occur as isometric grains 10–15 μm in size or angular, elongated inclusions up to 50 μm in size in pyrite and, rarely, quartz. *Nickeline* forms dissemination of oval grains less than 10 μm in size in quartz; it contains Fe (up to 3.4 wt%) and Co (1.5 wt%). Subisometric grains of *melonite* 10–30 μm in size or its intergrowths with gold were identified in pyrite from quartz veins in listvenites. The mineral contains 0.1 wt% Co. *Monazite* and *xenotime* were found as angular grains less than 10 μm in size in pyrite from black shales.

Gold occurs in both listvenites and carbonate–quartz veins in listvenites. In listvenites, it is observed as large (0.50–0.75 mm, rarely up to 1 mm) elongated or curved grains and microscopic (10–200 μm) crystals in quartz and pyrite, and at the contacts of quartz and carbonates (Fig. 6g and h). Small grains of gold are often associated with chalcopyrite. The Ag contents in gold vary from 0.27 to 8.96 wt% (Table 2). Gold also contains Cu (0.04–1.83 wt%) and Hg (0.01–0.48 wt%). Gold is mostly of high fineness (990–1000‰) (Fig. 7). In quartz veins from listvenites, gold grains up to 50 μm in size occur at the contacts of quartz and pyrite or are included in pyrite (Fig. 6g and h). In pyrite, gold may be intergrown with tetrahedrite or melonite (Fig. 6c). The composition of gold is similar to that from listvenites with the fineness maximum of

Table 1
Chemical composition of rocks of the Mechnikovskoe deposit, wt%.

SiO_2	TiO_2	Al_2O_3	Fe_2O_3	FeO	MnO	MgO	CaO	Na_2O	K_2O	H_2O^-	LOI	P_2O_5	Total
Porphyric plagioclase metabasalt													
53.69	0.81	18.96	3.60	3.59	0.13	2.95	5.10	5.29	2.11	0.10	2.54	0.62	99.49
52.00	0.81	19.52	3.07	3.86	0.13	2.89	4.40	5.10	3.03	<0.10	4.74	0.60	100.15
52.72	0.80	19.12	2.54	4.09	0.12	2.93	3.99	5.65	2.60	0.12	4.20	0.61	99.47
50.80	0.81	19.28	2.40	4.35	0.13	2.94	4.56	4.40	3.36	0.20	6.04	0.59	99.86
Metadiabase													
49.52	0.46	16.25	2.92	5.03	0.19	10.37	4.48	3.45	0.09	0.14	6.34	0.10	99.34
49.90	0.50	17.53	6.21	3.12	0.13	6.78	4.30	4.51	0.23	0.94	5.70	0.11	99.96
50.94	0.50	18.38	5.54	3.41	0.14	6.94	4.37	5.02	0.23	0.20	4.18	0.10	99.95
51.62	0.45	15.35	2.91	5.71	0.16	8.76	7.07	4.13	0.93	0.24	2.58	0.10	100.01
52.66	0.51	17.60	1.31	6.57	0.13	6.50	4.91	5.20	0.20	0.18	3.72	0.11	99.60
Quartz-carbonate-sericite metasomatite (beresite) (after volcanic rocks)													
43.21	0.43	13.91	3.88	3.77	0.12	7.63	7.08	0.34	4.42	0.48	14.34	0.07	99.68
45.38	0.54	14.02	5.77	2.33	0.13	5.30	6.53	0.55	4.52	0.30	14.40	<0.05	99.77
Granite													
71.32	0.22	16.51	1.02	0.61	0.02	0.51	0.20	4.62	2.97	0.18	1.48	0.25	99.91
72.12	0.25	16.30	0.96	0.78	0.01	0.60	0.14	3.54	3.63	0.14	1.50	0.12	100.09
72.06	0.23	16.51	0.56	0.96	<0.01	0.58	0.13	3.85	3.42	0.10	1.52	0.12	100.04
71.22	0.24	16.90	0.66	0.81	<0.01	0.66	0.14	3.61	3.76	0.10	1.72	0.15	99.97
72.98	0.22	15.53	1.03	0.54	<0.01	0.75	0.15	2.92	3.81	0.16	1.76	0.14	99.99
Sericite-quartz metasomatite (after granite?)													
58.08	0.55	18.96	9.38	0.99	0.14	0.38	0.26	2.96	3.49	0.64	4.04	0.10	99.97
Serpentinite													
40.30	0.05	0.84	5.49	2.62	0.11	37.90	0.30	0.05	0.03	0.38	11.86	<0.05	99.93
39.04	<0.05	0.54	6.67	2.06	0.09	38.47	0.37	0.08	<0.01	0.30	12.33	<0.05	99.95
Listvenite													
28.04	<0.05	0.80	0.77	4.07	0.07	30.18	1.30	0.05	0.20	0.80	33.74	<0.05	100.02
29.02	<0.05	0.40	0.63	5.03	0.03	29.51	0.40	0.95	0.12	0.46	33.42	<0.05	99.97
28.90	<0.05	0.69	1.66	4.31	0.19	28.56	1.91	0.16	0.24	0.26	33.06	<0.05	99.94
27.92	<0.05	0.68	1.27	4.07	0.12	32.95	0.30	0.56	0.01	0.29	31.88	<0.05	100.05
Carbonate-talc rock													
34.18	<0.05	0.83	3.12	3.95	0.13	34.98	0.76	0.60	<0.01	0.26	21.04	0.06	99.91
Detection limit, wt%													
0.8	0.05	0.05	0.05	0.1	0.01	0.01	0.01	0.01	0.01	0.1	0.1	0.05	
Analytical uncertainty, wt%													
±0.7	±0.08	±0.9	±0.3	±0.3	±0.03	±0.3	±0.2	±0.3	±0.3	±0.08	±0.2	±0.06	

940–950‰ (Table 2, Fig. 7). In beresites, gold was found as small (<10 μm) elongated and angular inclusions or veinlets in oxidized pyrite crystals (Fig. 6). The Ag contents, as well as the fineness, are similar to those of gold from listvenites and quartz veins (Table 2, Fig. 7). Gold in black shales is observed as small (up to 20 μm) oval and elongated inclusions and rare crystals in pyrite (Table 2, Fig. 6d and c).

Petzite crystals up to 5 μm in size are included in listvenites and pyrite, where they are often associated with galena (Fig. 6e and f). Subisometric grain of Au- and Ag-telluride ~2 μm across was found in quartz from listvenite matrix (Fig. 6i). The composition of mineral is close to that of *stutzite* $(Ag_{3.02}Au_{0.93}Cu_{0.12})_{4.07}Te_{3.00}$.

4.2.3. Fluid inclusion data

Primary and secondary fluid inclusions (FIs) were studied in the gold-bearing quartz from veins in listvenites. Primary FIs are subdivided on three- and two-phase inclusions (type 1 and type 2, respectively). Rare rounded, oval or irregular FIs of type 1 (10% of the total amount of FIs) are 10–20 μm in size, partly showing negative crystal shapes. They consist of a liquid, a vapor bubble and a liquid CO_2. The vapor bubble with liquid CO_2 occupies 20–40 vol% of the inclusions. The T_{mCO2} indicates the presence of CO_2 in the FIs (Table 3). Assuming the CO_2 density, the pressure of the fluid may be estimated at 0.4–0.8 kbar. These values are in agreement with those calculated using calcite–dolomite thermometer (Sazonov et al., 1999). The homogenization temperature (T_h) of FIs varies from 147 to 246 °C with an average of 217 °C, and the majority of values are in a range of 240–260 °C (Table 3). Taking into account the pressure of the fluid and corresponding pressure correction (~60 °C), the formation temperature is estimated to be of 207–306 °C. The T_m of −7.3 to 13.3 °C corresponds to the salinities of 10.6–16.7 wt% $NaCl_{eq}$, with an average value of 13.2 wt% $NaCl_{eq}$ (Table 3). Most salinity values are in range of 12.5–13.0 wt% $NaCl_{eq}$. The T_e (−20.3 to −23 °C) is close to the eutectic temperature of the NaCl–H_2O with possible presence of $NaHCO_3$ and KCl (cf., Borisenko, 1977).

Two-phase (light aqueous + dark vapor bubble) angular, oval and negative-shaped individual or grouped FIs of type 2 are 8–15 μm in size and compose up to 50% of the total amount of FIs. The vapor bubble occupies 15–20% of the inclusions. Cooling of some FIs results in formation of liquid CO_2. The T_h of FIs varies from 110 to 256 °C and the majority of values is in a range from 180 to 200 °C (Table 3). Pressure-corrected trapping temperatures are 170–316 °C. The T_m of FIs of −6.1 to −10.8 °C is indicative of salinities ranging from 9.1 to 14.3 wt% $NaCl_{eq}$ with an average value of 11.3 wt% $NaCl_{eq}$; most salinity values correspond to a range of 12.5–13.0 wt% $NaCl_{eq}$ (Table 3). The T_e of −20.8 to −22.9 °C is close to the eutectic temperature of NaCl–H_2O system with possible presence of $NaHCO_3$ and KCl (cf., Borisenko, 1977). The estimated density of the fluid is ~0.92 to 1.0 g/cm^3 (cf., Wilkinson, 2001).

Small (<10 μm) two-phase (light liquid + vapor bubble) secondary tubular FIs are associated with fine chains of small one-phase liquid inclusions, which cut several quartz grains. The vapor bubble in these FIs

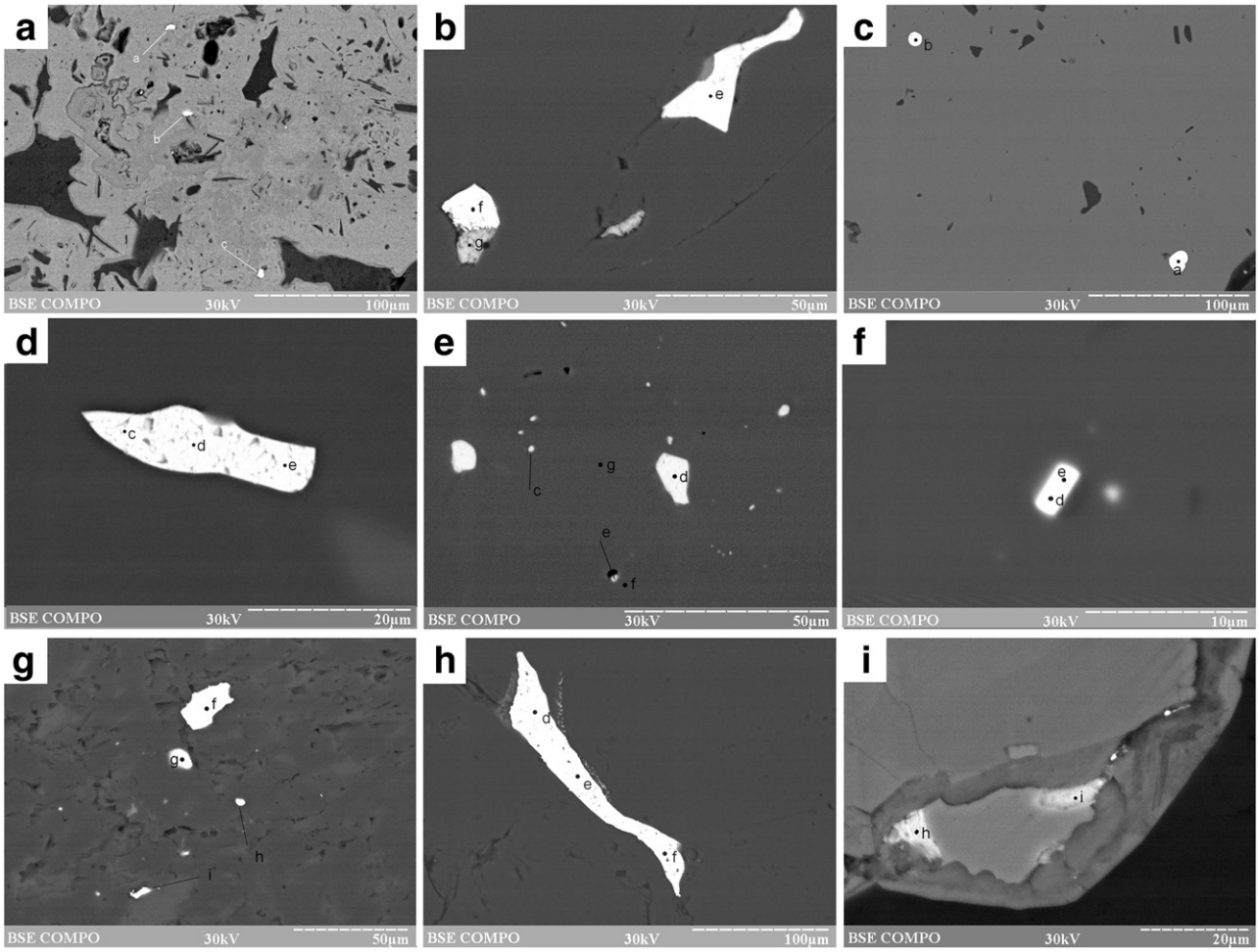

Fig. 6. Minerals of precious metals and some accessory ore minerals of the Mechnikovskoe deposit: (a) gold inclusion in goethite-replaced pyrite from beresites; (b) gold veinlet (point *e*) and intergrowth of gold (point *f*) and melonite (point *g*) in pyrite crystal from the quartz veinlet in listvenite; (c, d) inclusions of gold in pyrite crystals from black shales; (e) inclusions of petzite (points *c*, *e*) and galena (point *d*) in Ni-bearing pyrite (points *g*, *f*) from listvenites; (f) petzite crystal in listvenite; (g) inclusions of gold in listvenite; (h) gold veinlet in quartz from listvenite; (i) vague aggregates of iodargyrite in pyrite crystal replaced by goethite from beresites. SEM-photo.

occupies 5–20% of the inclusion. The FIs are homogenized in liquid and their T_h is much lower relative to the primary FIs (112–119 °C with an average of 115 °C, Table 3).

4.3. Altyn-Tash ore field, Altyn-Tash deposit

The Altyn-Tash deposit is situated 24 km south-southwest from the Mechnikovskoe deposit (59.93596° N, 54.70008° E). It has periodically been mined from the end of 19th to the middle of the 20th centuries. About 500 kg of gold was extracted from this deposit and its resource base is still considerable, which allows the YuzhUralZoloto Company to carry out the exploration works within the ore field using drilling.

4.3.1. Geological outline of the deposit

The deposit is located in the narrowest northern part of the MZ and is related to the foliated zone between two longitudinal normal–strike-slip faults, which are controlled by small lens-like bodies of serpentinites. The Altyn-Tash foliation zone is 100–300 m thick and longitudinally extended for 8 km. The area of the deposit is composed of basalts and basaltic andesites, which are transformed into sericite–quartz–chlorite ± albite and chlorite schists near the faults. The central part of the deposit contains the relics of primary volcanic rocks. The host rocks occur almost vertically and their occurrence is concordant with general foliation of the structure (Fig. 8). Plagiogranitic dikes at the deposit were described during exploration works (unpublished report of Lobanov, 1974), however, they lack support from the low SiO_2 content of the rocks (max 65 wt%). Later, all the light-colored rocks were ascribed to carbonate–quartz ± albite metasomatites (Sazonov et al., 1999). Four quartz vein zones associated with finely intercalated listvenites and quartz–carbonate–albite ± tourmaline metasomatites (beresites), were revealed within the deposit (Fig. 1a). The thickness of an alteration zone is ~50 m, which significantly exceeds that of the ore intervals. The average Au grade of ores is 5–6 g/t, going up to 19–25 g/t (unpublished report of Lobanov, 1974; Sazonov et al., 1999). Listvenite and metasomatites are composed of quartz, albite, carbonates (magnesite and dolomite), mica (sericite, paragonite and fuchsite) and, locally, chlorite, epidote and leucoxene. Ore minerals form scarce dissemination in metasomatites and compact pockets in vein selvages. The amount of ore minerals is generally very low.

4.3.2. Ore mineralogy

Pyrite, chalcopyrite and secondary copper sulfides are major ore minerals. Pyrite occurs as fine euhedral crystals in the rocks and contains 0.3–0.5 ppm of Au (INNA of pyrite monofractions). Pyrite from quartz veins contains 13–28 ppm Au (unpublished reports of Lobanov et al., 1974). Chalcopyrite and rare galena, sphalerite, pyrrhotite, tetradymite and gold form inclusions in pyrite. Rare minerals of

Table 2
Chemical composition of rocks of the Ganeevskoe deposit, wt%.

SiO_2	TiO_2	Al_2O_3	Fe_2O_3	FeO	MnO	MgO	CaO	Na_2O	K_2O	H_2O^-	LOI	P_2O_5	CO_2	Total
Metabasalts														
50.38	1.55	14.44	3.35	7.51	0.19	7.50	7.75	4.05	0.10	0.16	2.62	0.16	0.10	99.76
51.36	1.55	14.78	3.40	6.75	0.17	6.30	8.61	4.08	0.09	<0.10	2.10	0.18	0.10	99.37
52.88	0.92	16.08	3.28	7.58	0.20	5.00	6.26	4.39	0.26	0.16	2.24	0.16	0.10	99.44
Carbonatized and chloritized tuffites														
45.68	1.11	14.21	1.84	6.86	0.16	4.40	7.93	3.25	1.49	0.10	12.18	0.17	10.02	99.36
44.52	1.84	17.06	2.56	6.36	0.13	6.60	6.51	3.84	0.91	0.14	8.46	0.34	4.55	99.29
49.44	1.12	14.69	3.50	7.72	0.22	4.60	4.85	5.17	0.28	<0.10	7.60	0.20	5.94	99.42
44.72	0.97	13.89	1.46	7.33	0.24	6.20	7.35	3.56	1.00	<0.10	7.60	0.20	10.33	99.36
48.08	1.18	15.75	2.65	7.18	0.16	6.30	3.03	5.10	0.48	<0.10	9.06	0.36	4.22	99.36
45.78	0.87	15.42	1.16	7.44	0.15	6.70	6.17	3.50	1.22	<0.10	10.88	0.11	8.06	99.35
Carbonatized serpentinites														
40.52	0.12	14.27	1.94	5.82	0.17	12.60	10.6	1.92	0.48	0.14	10.76	<0.05	5.69	99.34
Listvenites														
24.02	0.05	0.68	0.07	4.96	0.11	28.00	6.23	0.04	0.14	<0.10	35.58	<0.05	18.98	99.56
30.02	0.05	0.52	0.43	4.69	0.09	30.00	0.86	0.04	<0.01	<0.10	32.96	<0.05	13.46	100.00
41.20	0.12	12.75	0.62	5.71	0.15	8.70	7.32	2.88	2.26	0.12	18.02	<0.05	4.18	99.88
Beresites														
46.86	1.00	13.23	3.09	4.92	0.16	4.70	5.59	7.95	0.24	<0.10	0.19	9.44	9.44	99.49
46.30	0.92	12.04	0.87	8.12	0.19	5.90	4.99	4.47	1.13	<0.10	0.13	10.46	10.46	99.40
45.19	1.66	12.39	0.81	5.70	0.13	5.57	6.86	4.74	1.55	0.20	14.28	0.54	11.75	99.62
Detection limit, wt%														
0.8	0.05	0.05	0.05	0.1	0.01	0.01	0.01	0.01	0.01	0.1	0.1	0.05	0.1	
Analytical uncertainty, wt%														
±0.7	±0.08	±0.9	±0.3	±0.3	±0.03	±0.3	±0.2	±0.3	±0.3	±0.08	±0.2	±0.06	±0.2	
*Gabbro (n 5)**														
46.79	1.30	16.58	10.36		0.14	7.82	7.13	3.58	1.10	n.a.	4.19	0.16	n.a.	100.07
*Subalcali gabbro (n 1)**														
53.55	1.02	18	8.82		0.09	3.6	5.26	5.4	0.8	n.a.	2.4	0.6	n.a.	99.54
*Gabbrodiorite (n 1)**														
56	0.68	17.4	5.44		0.07	3.2	6.25	5.4	0.56		56	0.68		100.21
*Diorite (n 1)**														
64	0.69	15.72	3.41		0.03	2.6	1.41	4.72	3.05		4.5	0.18		100.3

Note: *data of Znamensky et al. (2014).

quartz veins include arsenopyrite, sphalerite, galena, molybdenite, tennantite, bornite, aikinite, tetradymite, tellurobismuthite, altaite, melonite, frohbergite, native tellurium, millerite, gersdorffite, linnaeite, Co–Ni-bearing pyrite, pentlandite, native gold, electrum, and hessite (petzite?) (Melekestseva et al., 2011 and reference therein).

Visible gold grains up to 0.5 mm in size were found in the sulfide–ankerite–quartz vein (0.5 m thick) in the southeastern part of the deposit (Melekestseva et al., 2011). They are xenomorphic relative to host minerals and contain 10.92–13.03 wt% Ag (Fig. 9, Table 2). Microscopic gold grains are up to 30 μm in size and occur at the contacts of quartz and oxidized sulfides, or as inclusions in fully oxidized sulfide veinlets with relict pyrite and chalcopyrite. This gold contains 14.2–23.5 wt% Ag. Very small (up to 10 μm in size) and finely dispersed probably supergene gold grains with vague boundaries are dispersed in fractures of goethite aggregates. This gold is almost pure (0.18 wt% Ag was detected in one of five analyses). The composition of gold from this deposit exhibits the largest variations in terms of Au, Ag, Cu and Hg contents in comparison with the other studied deposits (Table 2).

In beresites, gold grains are up to 0.6 mm in size, and characterized by platy, cleaved and dendritic shapes. They are intergrown with sericite, quartz, and dolomite, as well as occur as inclusions in pyrite (1–5 μm in size). Locally, gold hosts the inclusions of the rock-forming minerals.

4.3.3. Fluid inclusion data

Three types of FIs were distinguished in the gold-bearing quartz of the deposit. The overwhelming majority of the FIs is represented by primary two- and three-phase (vapor + liquid) inclusions with size of 3–20 μm (rarely, 7–12 μm), where vapor bubble occupies 70–80 vol% (type 1). Rare three-phase inclusions contain liquid CO_2 in the vapor bubble. The FIs of type 1 are evenly distributed in quartz grains and form groups of three to five inclusions. They are characterized by rounded to oval, irregular or, locally, negative-crystal shape. The FIs are homogenized in vapor at temperatures of 229–294 °C with maximum of 240–250 °C. The T_{mCO2} of the FIs shows that the vapors are dominated by CO_2 and probably indicates the presence of some amount of CH_4 (T_{mCO2} less than −56.6 °C) (Table 3). The dark color of most inclusions prevented accurate measurement of their T_m, however, two lighter FIs exhibited T_m of −1.3 and −1.6 °C, which corresponds to the salinity of the fluid of 2.2–2.4 wt% NaCl-equiv. (Bodnar and Vityk, 1994). Their T_e (−21.4 to −21.2 °C) is close to that of the NaCl–H_2O system (cf., Borisenko, 1977). The density of the fluid is ~0.86 g/cm^3.

Much rarer primary two-phase (liquid + vapor) FIs are 8–10 μm in size (type 2) and show slightly elongated shape. They consist of a light liquid and a vapor bubble, which occupies 10–20 vol% of the inclusions. Some of the FIs are three-phase, where vapor bubble occupies up to 30 vol% of the inclusions and contains liquid CO_2. The FIs of type 2 are evenly distributed in quartz grains. Similarly to FIs of type 1, the T_{mCO2} of the FIs shows that vapors are dominated by CO_2 and probably indicates the presence of some amount of CH_4 (Table 3). The T_h of these FIs is 214–301 °C with maximum of 270–290 °C. The T_m of this FI type varies from −7 to −13.2 °C (Table 3). According to Bodnar and Vityk (1994), these values correspond to salinities of 9.8–16.6 wt% NaCl-equiv. with maximum of 14–15 wt% NaCl-equiv. The temperature

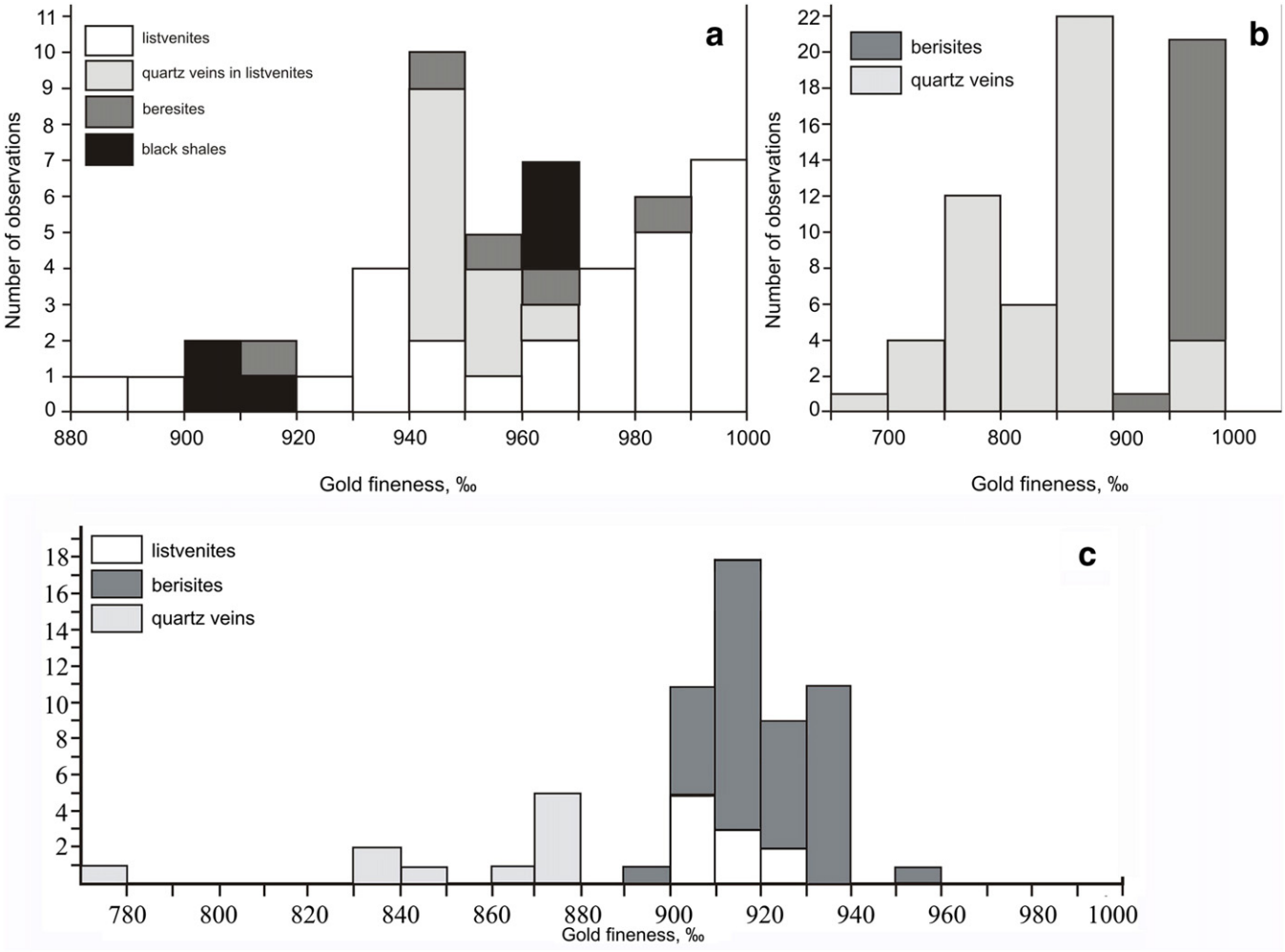

Fig. 7. Gold fineness. Deposits: a – Mechnikovskoe, b – Altyn-Tash, c – Ganeevskoe.

Table 3
Composition of gold of Mechnikovskoe, Altyn-Tash, and Ganeevskoe deposits (wt%).

	Au	Ag	Cu	Hg	Total
Mechnikovskoe deposit					
Listvenites	96.30	3.07	0.41	0.09	99.87
(n = 28)	88.42–99.53	0.27–8.96	0.00–1.83	0.00–0.48	99.53–100.06
Beresites	95.02	4.7	–	–	99.76
(n = 5)	90.75–98.14	1.66–8.95			99.52–99.94
Black shales	93.52	5.85	0.38	0.11	99.86
(n = 6)	90.03–96.38	2.79–9.24	0.25–0.53	0.00–0.32	99.68–100.07
Quartz veins in listvenites (n = 13)	94.95	4.31	0.25	0.31	99.82
	94.03–96.11	3.32–5.25	0.00–0.48	0.00–1.39	99.47–99.97
Altyn-Tash deposit					
Beresites (n = 18)	96.10	3.74			99.86
	93.09–97.48	1.74–6.91			99.56–100.06
Quartz veins (n = 50)	84.08	14.01	1.74	0.06	99.86
	66.76–98.04	0.00–23.5	0.28–10.76	0.00–0.53	99.56–100.06
*Ganeevskoe deposit**					
Listvenites (n = 10)	91.35	8.65		–	100
	90.26–92.63	7.37–9.74			
Beresites (n = 41)	92.07	7.93		–	100
	89.6–95.78	4.22–10.4			
Quartz vein (n = 8)	84.79	15.21		–	100
	77.03–87.87	12.13–22.97			

Notes: n, number of analyses; dash, not detected; numerator, average value; denumerator, min to max values; *, the total is recalculated to 100%.

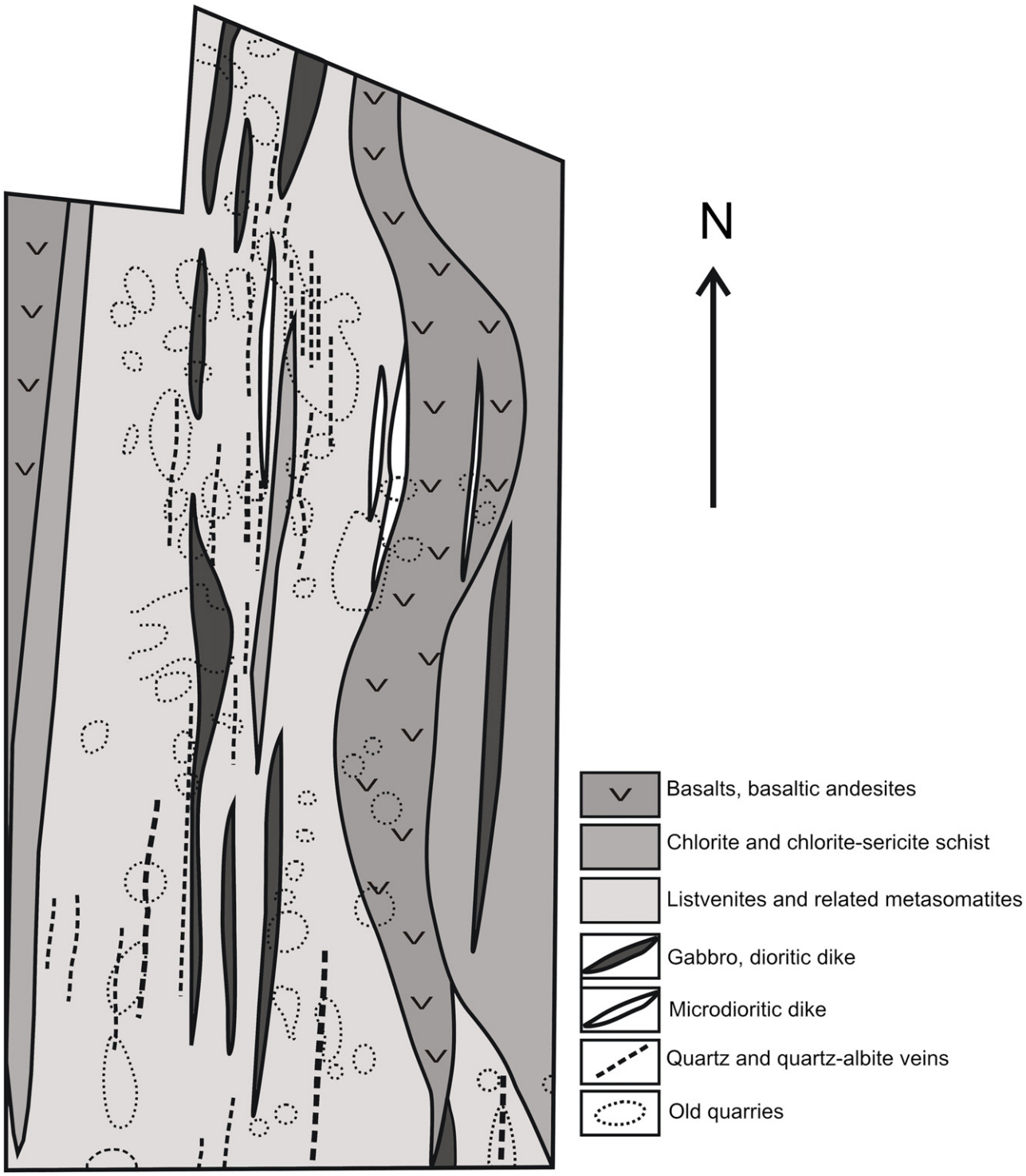

Fig. 8. Geological structure of the Altyn-Tash deposit, simplified after Sazonov et al. (1999).

vs. salinity dependence is slightly negative. The T_e corresponds to that of the NaCl–H_2O system and shows a small maximum in range of −21.8 to −22.0 °C, which may indicate the presence of $NaHCO_3$ (cf., Borisenko, 1977). The density of the fluid is ~0.83–0.97 g/cm^3.

The density of the fluid for both types of FIs can be estimated at 1.1–1.4 kbar, corresponding to depth of ~4–5 km. The temperatures of mineral formation are close to those of T_h of the FIs on the basis of similar range of T_h of coexisting FIs of types 1 and 2 (cf., Bortnikov et al., 1998).

The FIs of type 3 include small (5–7 μm in size) primary–secondary and secondary two-phase (liquid + vapor) inclusions of tubular shape; the vapor bubble occupies 5–10 vol% of the inclusions. They occur among the chains of small secondary one-phase liquid inclusions, which cut several grains. The T_h of type 3 FIs is 118–285 °C, with two small maximums at 270–280 and 220–230 °C.

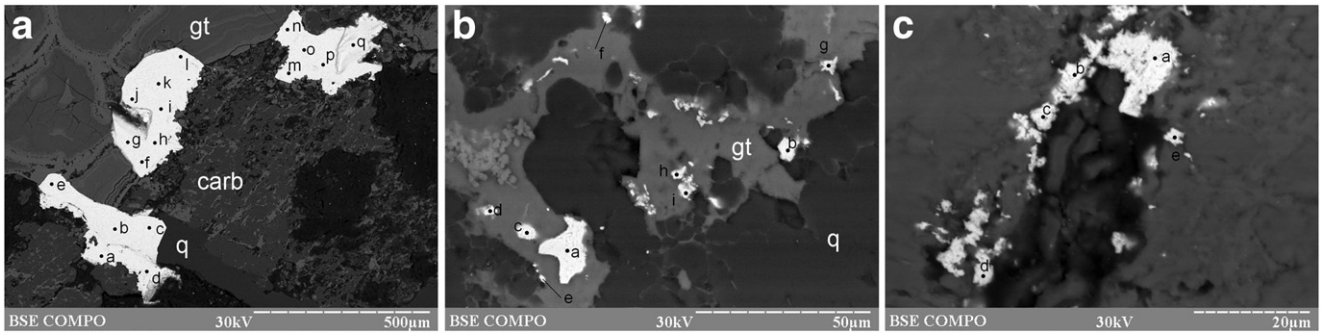

Fig. 9. Native gold of the Altyn-Tash deposit: a) gold with low Cu (up to 0.45 wt%) and Hg (up to 0.53 wt%) contents at the contact of quartz (q), carbonates (carb), and goethite (gt); b) Hg-free Cu-bearing (2.12–5.75 wt% Cu) gold in goethite–quartz aggregate; c) supergene (?) Cu-bearing (up to 10.76 wt% Cu in point *e*) in goethite. SEM-photo.

4.4. Buyda ore field, Ganeevskoe deposit

The Buyda ore field includes Ganeevskoye and Oktyabr'skoe listvenite-related gold deposits, as well as a series of smaller lode quartz vein occurrences (Fig. 10).

4.4.1. Geological outline of the deposit

The deposit is situated in the northern part of the MZ, 9 km southeast of the town of Uchaly (59.48409° N; 54.23529° E) (Fig. 11). It was first mined in 19th–the beginning of the 20th century by small quarries, and most recently in 2010–2012 by the Bashkir Gold Company by an open pit. The deposit is situated within the Karagayly longitudinal steep fault zone and is covered by residual talus up to 20 m thick. The structure of the deposit is a result of development of the shear extension duplex (Znamensky et al., 2014).

The eastern flank of the deposit is composed of metabasalts of the Early Silurian Polyakovka Formation, and quartz–chlorite schists developed after volcanic and volcanoclastic rocks near the faults (Fig. 11). Near the ore zone, schists are significantly carbonatized. A lens of talc-bearing serpentinites is traced in the weathered clayey rocks developed after volcanics. The western flank of the deposit is composed of quartz–chlorite schists after volcanoclastic rocks, probably of the Karamalytash Formation, and host thin tectonic lenses of serpentinites with talc and chlorite; these rocks have contact with metabasalts in the north (Fig. 11). Znamensky et al. (2014) described a tectonic sheet of gabbro and dikes of subalkaline gabbroic rocks in the area of the deposit. Small subvolcanic bodies of non-mineralized gabbrodiorites and diorites occur in the area of the deposit. The large Akhunovo gabbro–tonalite–granitic pluton (Figs. 1 and 11) is located at 5 km east. The age of gabbro–diorite–granite magmatism is a matter of debate. On the basis of zircon ages and geochemistry of rocks, the formation of this pluton is related to the beginning of the arc-continent collision (Late Devonian–Early Carboniferous) (Fershtater, 2013). However, in the majority of published maps, its age is accepted as Late Carboniferous.

The 5–30-m thick ore zone is exposed in the axial part of the open pit. It includes pyrite-bearing sericite–quartz–carbonate–albite and fuchsite–quartz–carbonate metasomatites (beresites and listvenites, respectively) with minor quartz veins. The rocks are strongly deformed and characterized by abundant boudinage structures. No granitic rocks were found in the structure of the deposit.

Listvenites with schistose, banded or massive structures are often cut through by thin quartz and quartz–albite veins. They are mostly composed of carbonates (dolomite and magnesite in various proportions), quartz and albite, subordinate fuchsite and pyrite, and rare paragonite, chalcopyrite and gold. Listvenites are characterized by low SiO_2, Al_2O_3 and TiO_2 contents, significantly variable CO_2 contents, high contents of alkalis (especially Na_2O) relative to the parental rocks (Table 4) and increased contents of typical ultramafic Cr (172–340 ppm) and Ni (83–1544 ppm), although no chromite was found under the microscope. The Au grades reach 10 g/t.

Beresites are mostly schistose, rarely massive rocks, consisting of carbonates (dolomite, ankerite and, locally, Fe-magnesite), quartz, albite, sericite and rare chlorite. They host thin quartz, quartz–carbonate and quartz–albite veinlets. Beresites of this deposit are distinct from classical beresites of the Berezovskoe deposit (Sazonov, 1984) in the higher amount of albite, which may be dominant over quartz and sericite. The ore minerals are pyrite, chalcopyrite and native gold. Pyrite forms cubic crystals up to a few millimeters in size, often with inclusions of gold. In comparison with listvenites, beresites contain elevated amounts of SiO_2, Al_2O_3 and TiO_2 and correspond to volcanoclastic mafic rocks by chemical composition (Table 4). The increased Cu contents (114–241 ppm) are comparable with those of altered tuffites of the ore zone. The Au grades of beresites are up to 18 g/t.

Quartz veins 1–7 m thick occur at the contact of listvenites and chlorite schists. Quartz and albite also form thin veinlets in metasomatites of the ore zone. Quartz veins typically host dolomite, rare sulfides, native gold and Au- and Ag-tellurides with inclusions of gold. The Au grades in the thickest quartz veins are 1–3 g/t.

4.4.2. Ore mineralogy

Pyrite is a major ore mineral of the deposit; rutile, magnetite, hematite and goethite are also abundant. Accessory and rare minerals include chalcopyrite, galena, pyrrhotite, sphalerite, nickeline, fahlores, native gold and Au- and Ag-tellurides.

Pyrite in listvenites and beresites forms dissemination of cubic crystals and their aggregates up to 3 mm in size. It is also abundant in carbonate–chlorite schists after tuffites in the ore zone. Pyrite from listvenites and beresites contains inclusions of chalcopyrite, pyrrhotite, galena, sphalerite, magnetite, gold (Fig. 12) and non-opaque minerals; the orientation of latter is parallel to schistosity. Pyrite is often corroded and fractured and, locally, gold is confined to fractures.

Chalcopyrite forms anhedral interstitial aggregates 0.2–0.5 mm in size between non-opaque minerals in beresites, listvenites and quartz veins. It may also be found as single inclusions in pyrite or as intergrowths with it. Chalcopyrite from quartz veins contains up to 1.84 wt% Ni. *Pyrrhotite* occurs as anhedral aggregates in quartz or isometric inclusions up to 20 μm in size in pyrite from listvenites and beresites. Inclusions of *galena, sphalerite* and *tennantite* 1–20 μm in size are mainly hosted in pyrite, rarely forming intergrowth with chalcopyrite.

In thick quartz veins, abundant galena is associated with tennantite, aikinite, polydymite, millerite, gold and tellurides (Fig. 12c–e). It forms

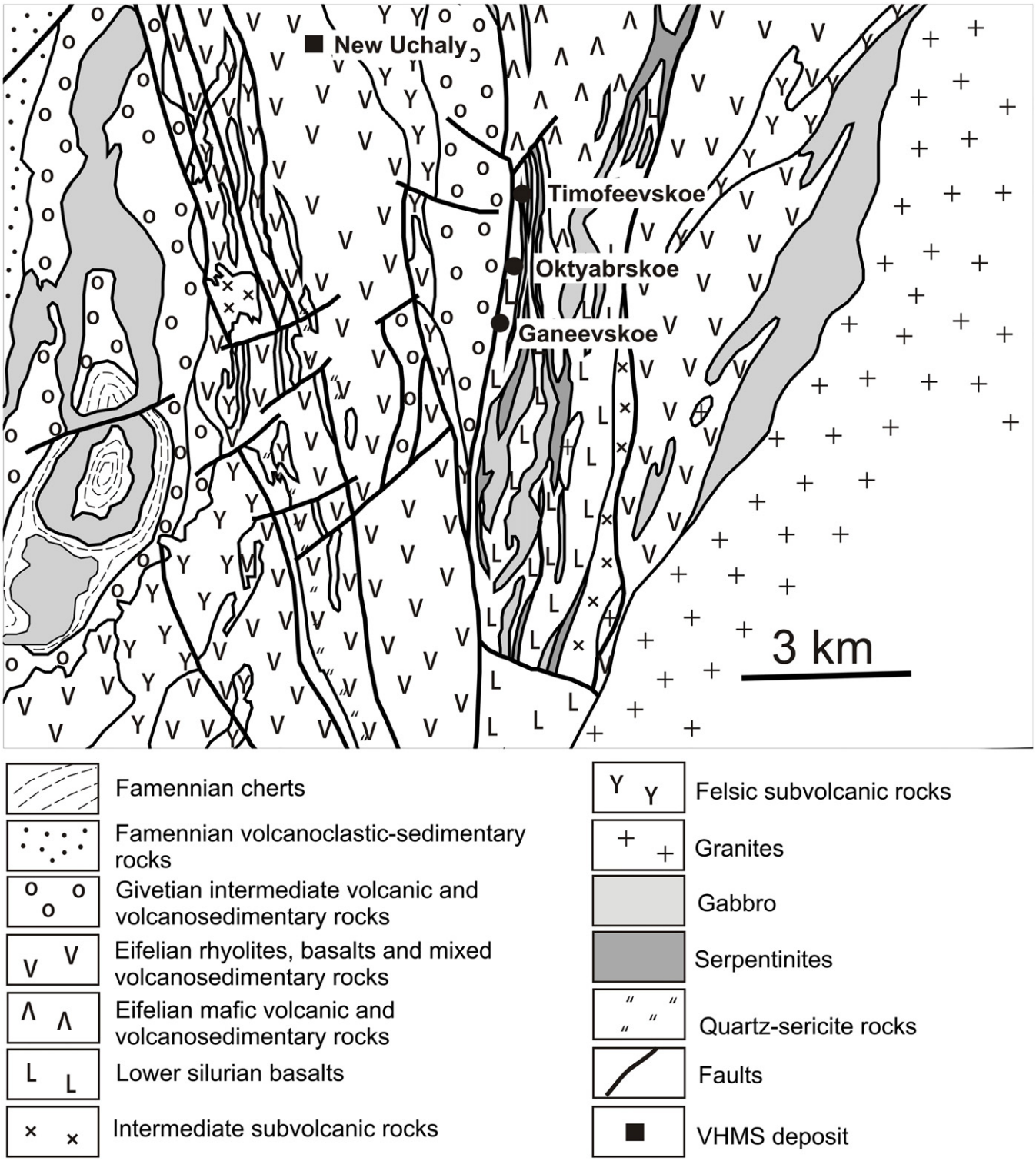

Fig. 10. Geological structure of the Buyda ore field, simplified after unpublished report of Gavrilov et al. (2001).

large (0.1–1.0 mm) euhedral and subhedral cubic crystals with inclusions of aikinite (Fig. 12e), tellurides and gold and contains (wt%) Ag (up to 2.31) and Bi (up to 5.08) and, rarely, Fe (up to 0.20).

Tennantite from quartz veins is intergrown with chalcopyrite and contains (wt%) Hg (3.43), Cd (1.64), Ni (0.47) and Sb (1.65). *Aikinite* is intergrown with galena, hessite and petzite (Fig. 12f). Its chemical composition is rather variable and individual grains contain Fe (up to 4.00 wt%) and Ni (up to 0.76 wt%). *Polydymite* was found in heavy concentrate and is characterized by lamellar *millerite* lattice (Fig. 12f). Both minerals contain Co (7.59 and 1.57 wt%) and Fe (0.90 and 0.23 wt%), respectively. *Magnetite* and *hematite* occur as subhedral and, rarely, euhedral inclusions up to 30 μm in size in pyrite.

Native gold is found in listvenites, beresites and quartz, as well as carbonate–quartz–chlorite metasomatites after tuffites in the ore zone.

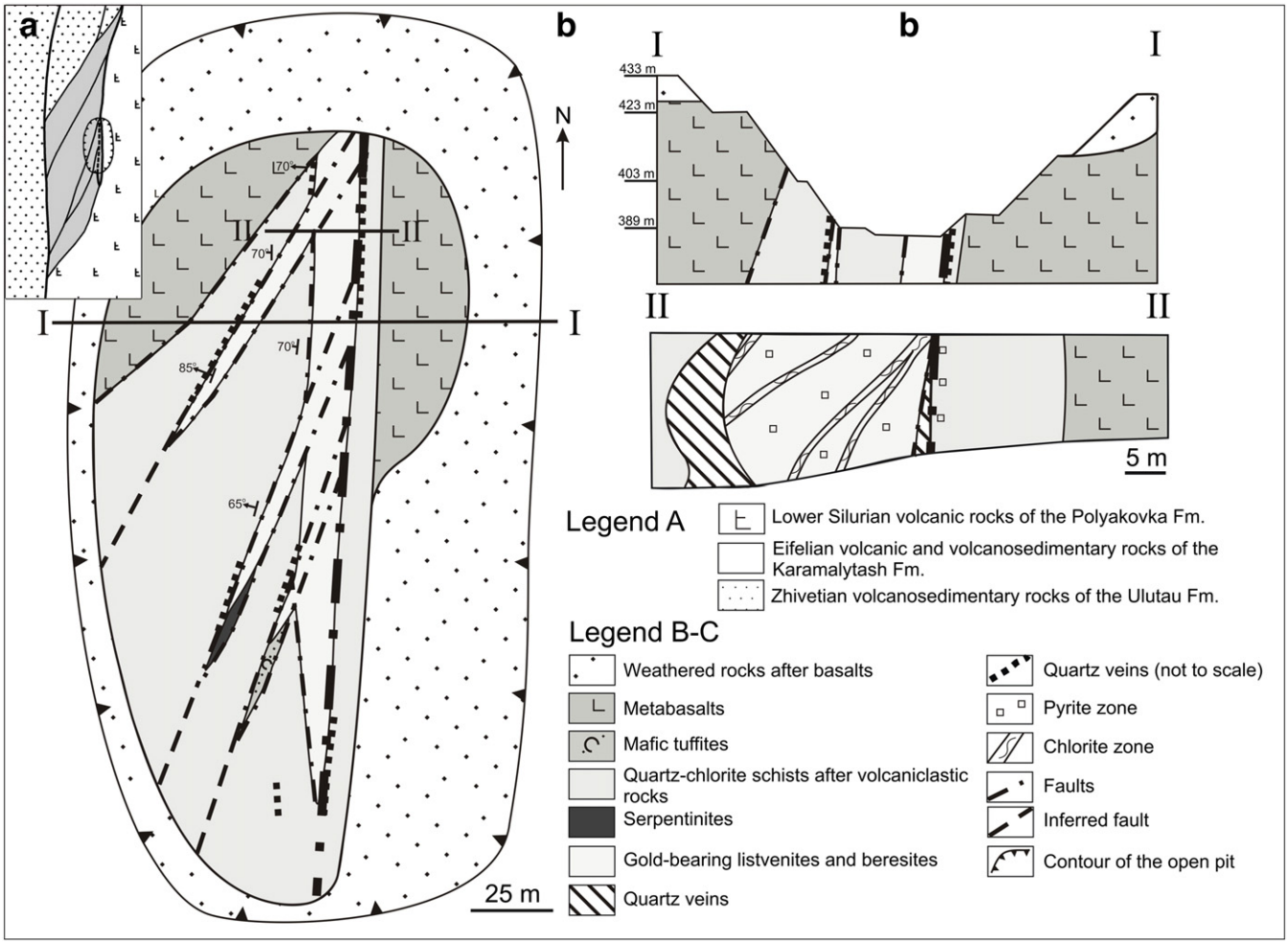

Fig. 11. Tectonic scheme after Znamensky et al. (2014) (a), simplified geological scheme (b) and cross-section along the profile I-I (c) of the Ganeevskoe deposit, composed by M.V. Zabotina and K.A. Novoselov.

In listvenites and beresites, gold occurs as: (1) elongated, oval and intricate inclusions ranging in size from 3 to 60 μm within pyrite and goethite (Fig. 12a, b); (2) subisometric, elongated or angular inclusions up to 0.1 mm, and (3) veinlets up to several millimeters long in quartz (Fig. 12h, i). The composition of gold from beresites and listvenites is similar. Gold is characterized by the presence of up to 11 wt% Ag, which is slightly higher relative to that from the Mechnikovskoe deposit (Table 2). In quartz veins, gold occurs as laths-like grains, leafs and dendrites and forms intergrowths with galena and complex inclusions in tellurides. The gold grains in quartz veins are 30 μm to 0.5 mm in size, in contrast to smaller gold grain included in sulfides or intergrown with galena (10–60 μm). The fineness of gold from quartz veins is lower in comparison with that from beresites and listvenites (Table 2).

Petzite and *hessite* were identified only in quartz vein. They form inclusions and intergrowths with galena, and often contain inclusions of gold (Fig. 12f and e).

4.4.3. Fluid inclusion data

Primary and secondary FIs were found in quartz from the carbonate–quartz veinlets in gold-bearing listvenites and beresites. Primary FIs 6–12 μm in size can be subdivided on three- and two-phase inclusions. The three-phase FIs consist of a light liquid, a dark liquid and a vapor bubble, which occupies ~20% of the inclusion. The two-phase (light liquid + vapor bubble) FIs are oval, angular and, locally, negative-shaped. The vapor bubble occupies 20–40% of the inclusions. T_{mCO2} indicates that the vapor phase is dominated by CO_2 (Table 3). Both types of FIs are homogenized in liquid phase and their T_h is similar, ranging from 140 to 340 °C, with an average of 243 °C and maximum abundance in a range of 240–260 °C (Table 3). The T_m of FIs varies from −1.0 to −10.0 °C, which corresponds to salinity values of 2.3–13.6 wt% $NaCl_{eq}$ with an average value of 8.5 wt% $NaCl_{eq}$ and maximums of 4–5 and 6–7 wt% $NaCl_{eq}$ (Table 3). The pressure of the fluid is estimated at 0.6–1.3 kbar, a pressure correction is +85 °C and pressure-corrected trapping temperatures are 282–327 °C. The T_e of FIs varies from −21.0 to −26.4 °C, which is close to that of the NaCl–H_2O system with small amount of KCl (cf., Borisenko, 1977).

Only two-phase primary FIs (5–8 μm in size), consisting of a light liquid and a vapor bubble, were found in quartz from beresites. The FIs were homogenized in liquid at T_h in a range from 117 to 373 °C, with an average of 221 °C. The most T_h values fall to the range of 240–260 °C, which is almost identical to those in listvenites (Table 3). The very small size of the FIs prevented accurate measurement of their T_m and T_e. Mostly one-phase (liquid) secondary FIs in quartz from both rock types are small (<5 μm in size), and were ignored from this study because of their size. The formation temperatures may be also estimated using chlorite thermometer (Cathelineau, 1988).

Table 4
Fluid inclusion data of gold-bearing quartz from the Mechnikovskoe, Altyn-Tash and Ganeevskoe deposits.

FI types	T_h, °C	T_e, °C	T_m, °C	Salinity, wt% NaCl-eq.	T_{hCO2}, °C	T_{mCO2}, °C	CO_2 density, $м^3/кг$	Pressure, kbar	Tf, °C
Mechnikovskoe deposit									
Primary three-phase in listvenites	147–246 217 ± 32 (n = 14)	−20.3…−23.0 −21.6 ± 0.7 (n = 14)	−7.3…−13.3 −9.7 ± 1.6 (n = 14)	10.6–16.7 13.2 ± 1.6 (n = 14)	27.3–31.3 28.7 ± 1.2 (n = 12)	−56.7…−54.3 −55.1 ± 1.38 (n = 3)	1.47–1.54	0.4–0.8	207–306
Primary two-phase in listvenites	110–256 181 ± 32 (n = 85)	−20.8…−22.9 −21.6 ± 0.6 (n = 17)	−6.1…−10.8–8.1 ± 1.2 (n = 20)	9.1–14.3 11.3 ± 1.5	–	–	–	–	170–316
Secondary two-phase in listvenites	112–119 115 ± 3 (n = 4)	–	–	–	–	–	–	–	–
Altyn-Tash deposit									
Primary two-phase vapor in listvenites	229…294 254 ± 17 (n = 41)	−21.4…−21.2 −21.3 ± 0.1 (n = 2)	−1.6…−1.3 1.45 ± 0.2 (n = 2)	2.2–2.4 2.3 ± 0.1 (n = 2)	8.4–17.8 13.1 ± 6.6 (n = 2)	−57.1…−54.2 −56.1 ± 0.8 (n = 18)	1.16–1.30	1.1–1.4	229–294
Primary two-phase liquid in listvenites	214–301 260 ± 25 (n = 51)	−20.5…−22.5 −21.3 ± 0.4 (n = 49)	−7…−13.2 −8.7 ± 3.6 (n = 49)	9.8–16.6 13.6 ± 1.9 (n = 49)	12.9–17.3 15.3 ± 1.6 (n = 10)	−57.2…−54.3 −55.1 ± 2.2 (n = 6)	1.20–1.28	1.2–1.5	214–301
Secondary two-phase liquid in listvenites	118–285 227 ± 44 (n = 22)	–	–	–	–	–	–	–	118–285
Ganeevskoe deposit									
Primary in listvenites	150–329 243 ± 36 (n = 52)	−21.0…−26.4 −23.2 ± 1 (n = 40)	−1.0…−10.0 −4 ± 1.9 (n = 32)	2.3–13.6 8.5 ± 3.3 (n = 32)	9.0–29.4 22.3 ± 6.2 (n = 21)	–	1.15–1.51	0.65–1.3	282–327
Primary in beresite	117–373 221 ± 57 (n = 103)	–	–	–	–	–	–	–	–

Notes: See text for abbreviations; n, number of analyses; dash, not analyzed; numerator, min to max values; denominator, average value and standard deviation.

Application of this thermometer yields the temperatures range from 290 to 330 for listvenites and from 310 to 330 °C for beresites, which is in agreement with fluid inclusion data.

4.5. Mindyak ore field, Mindyak deposit

The extraction of gold at the Mindyak deposit has begun at 1843. Fifteen mines have been opened in the next three decades. The primary gold has been extracted from 1934 to 1997. There are no precise data on the amount of gold extracted, but the proved reserves of the deposit are 1.5 t (http://mindyak.narod.ru/simple.html).

The deposit is located within the MUF (58.80924° N; 54.01342° E) and is hosted by an assemblage of tectonic sheets composed of the Eifelian porphyritic pyroxene–plagioclase basalts and their tuffs, Tournaisian–Visean limestones and their breccias, mélange serpentinites, carboniferous–siliceous shales and various olistostromes (Znamensky and Michurin, 2013). In the west, the tectonized ore-hosted sequence is thrust on the gabbro–diabase complex of unknown age and the rocks of the Mindyak ultramafic massif. No felsic to intermediate intrusive rocks were found in the area of the deposit (Fig. 13). The tectonic pattern of the deposit is a result of interception of the northeastern thrust and late zone of longitudinal small-amplitude strike-slip and oblique faults. The local structural control is related to shear deformations (Znamensky and Michurin, 2013).

The stockwork ore bodies are composed of quartz veins, which are mostly confined to the polymictic olistostrome, consisting of fragments of serpentinites, pyroxenites, hornblende gabbro and diabases with pillow structures (Znamensky and Michurin, 2013). The formation of quartz veins was accompanied by listvenitization and sulfidization of diabases, ultramafic rocks and shales. The variable economic Au grades are related to disseminated pyrite and quartz–sulfide veinlets. Quartz, albite and carbonates are the major minerals of metasomatites, which have been developed after all the varieties of rocks. Listvenites after ultramafic rocks contain Fe-bearing magnesite and fuchsite in contrast to carbonates of the dolomite–ankerite series and sericite in metasomatites after diabases and shales. Pyrite is a major ore mineral and its amount attains 5–7%. Chromite was locally found in listvenites.

Two stages of ore formation are distinguished at the deposit: the formation of disseminated ores and veins. The ore minerals of the first stage include pyrite and rare arsenopyrite, as well as gersdorffite and millerite in listvenites. Pyrite, chalcopyrite, pyrrhotite, sphalerite, tetrahedrite, ullmannite and breithauptite were formed at the second stage. Native gold is found in minerals of both stages. Pyrite is characterized by the increased Au contents: 10–100 ppm (70%) and more than 100 ppm (30%). Pyrite of the first stage is zonal and contains up to 5.34 wt% As. The gold fineness is 903–908‰ (Murzin et al., 2001 and reference therein). The ore formation conditions were estimated on the basis of calcite–dolomite geothermometer: T = 340–450 °C and p = 0.55–0.66 kbar for the first stage, decreasing to T = 195–205 °C and p = 0.04–0.13 kbar for the second stage (Murzin et al., 2001).

4.6. Karan–Alexandrovsky ore field, Alexandrovskoe deposit

The Alexandrovskoe deposit (59.63169° N; 54.61753° E) is part of the Karan–Alexandrovsky group of the deposits, which is located in the MUF. The Paleozoic volcanic and volcanosedimentary rocks form a series of tectonic sheets of the northeastern strike. The presence of numerous ultramafic massifs and mélange zones

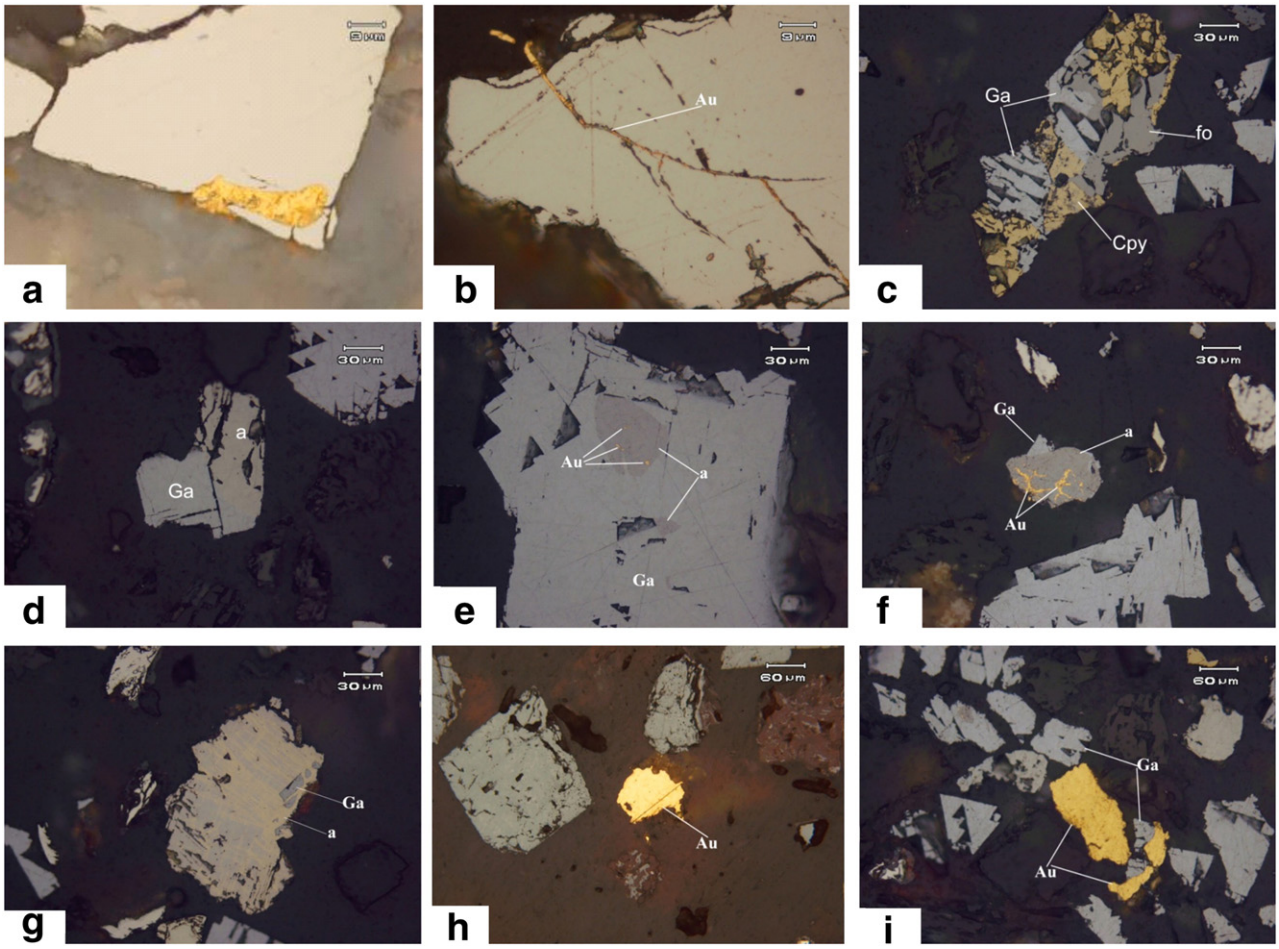

Fig. 12. Gold and rare minerals from beresites (a, b), quartz veins (c–g, i) and listvenites (h) of the Ganeevskoe deposit: (a) inclusions of gold in pyrite; (b) veinlet of gold in pyrite; (c) aggregate of galena with fahlore (fo) and chalcopyrite (Cpy); (d) aggregate of aikinite (point a) and galena; (e) hessite (point *a*) with inclusions of gold in galena crystal; (f) gold–petzite veinlets in hessite (point *a*); (g) lamellar millerite in polydymite; (h) gold grain in quartz (Au); (i) intergrowth of gold and galena (Ga) from quartz vein. Reflected light. Photos (b, c) polished section, others – heavy concentrates.

is related to the evolution of the MUF. The intrusive rocks include Ordovician to Devonian mafic and intermediate subvolcanic rocks and Middle Carboniferous to Early Permian granitosyenitic rocks of the Balbuk complex. The gold–quartz veins occur in serpentinites (Leont'evskoe, Sana Bukan-1, Mayak-2, South Muldakaevo occurrences). Some gold ore bodies of this area are confined to the contacts between various volcanic rocks and serpentinites (e.g., Alexandrovskoe, Borisovskoe) (Fig. 14). The ore bodies in some small gold deposits and occurrences (e.g., Maly Karan) are confined to the zones of albite metasomatites with gold-bearing sulfide–albite–quartz veins. The age of albitites of 266 ± 11 Ma (Znamensky et al., 2014) from the central zone of the Maly Karan deposit is in agreement with that of the Balbuk complex.

The Alexandrovskoe deposit was discovered in the 1880 s. It is confined to the tectonic contacts of schists and a sequence made up of basalts, siliceous shales and clayey–siliceous shales of the Silurian Polyakovka Formation. The serpentinite bodies also occur at this contact zone. The NE- and sN-trending ore bodies are almost vertical zones of disseminated sulfides in foliated listvenitized, chloritized and sericitized rocks and talc–carbonate metasomatites. The length of the ore bodies along the strike is up to 370 m, their thickness is 3–4 m and the average Au grade is 4 g/t. Pyrite is a major ore mineral. The ores contain 2–10.6 g/t Au, up to 1.63% Cu, 0.18–0.3% Zn and 5.63–12.7% Fe.

5. Oxygen, carbon, and sulfur isotopic composition of minerals

The oxygen isotopic composition of quartz from the Mechnikovskoe and Altyn-Tash deposits varies from 14.7 to 15.4‰ and 13.2 to 13.6‰, respectively (Table 5). The $\delta^{18}O$ values of quartz from beresites and listvenites of the Ganeevskoe deposit are almost identical and range from 12.6 to 12.7‰; the $\delta^{18}O$ value of quartz from galena- and telluride-bearing vein is slightly lower (12.0‰), and that of albite from beresites is furthermore lower (10.1‰).

In the Mindyak deposit, the carbon and oxygen isotopic composition of early carbonates from the ore-bearing metasomatites is −7.8 and +18.4‰, respectively, whereas the $\delta^{13}C$ and $\delta^{18}O$ values of late carbonates show a wide range from −21.6 to −6.1‰ and from +18.3 to +28.5, respectively (Murzin et al., 2002). In contrast, the carbon and oxygen isotopic composition of early carbonates from barren metasomatites exhibit narrower range of values: +1.08 to +6.26 and +19.32 to +22.86‰, respectively. The $\delta^{13}C$ and $\delta^{18}O$ values of late carbonates from barren metasomatites almost similar to those of early carbonates: −4.27 to +1.39 and +18.5 to +23.66‰, respectively.

The sulfur isotopic composition was analyzed in pyrite of the Mindyak (Golub et al., 1982; Znamensky et al., 2014) and Ganeevskoe (Znamensky and Michurin, 2013) deposits. The nodular diagenetic pyrite from host black shales of the Mindyak deposit has negative $\delta^{34}S$ values varying

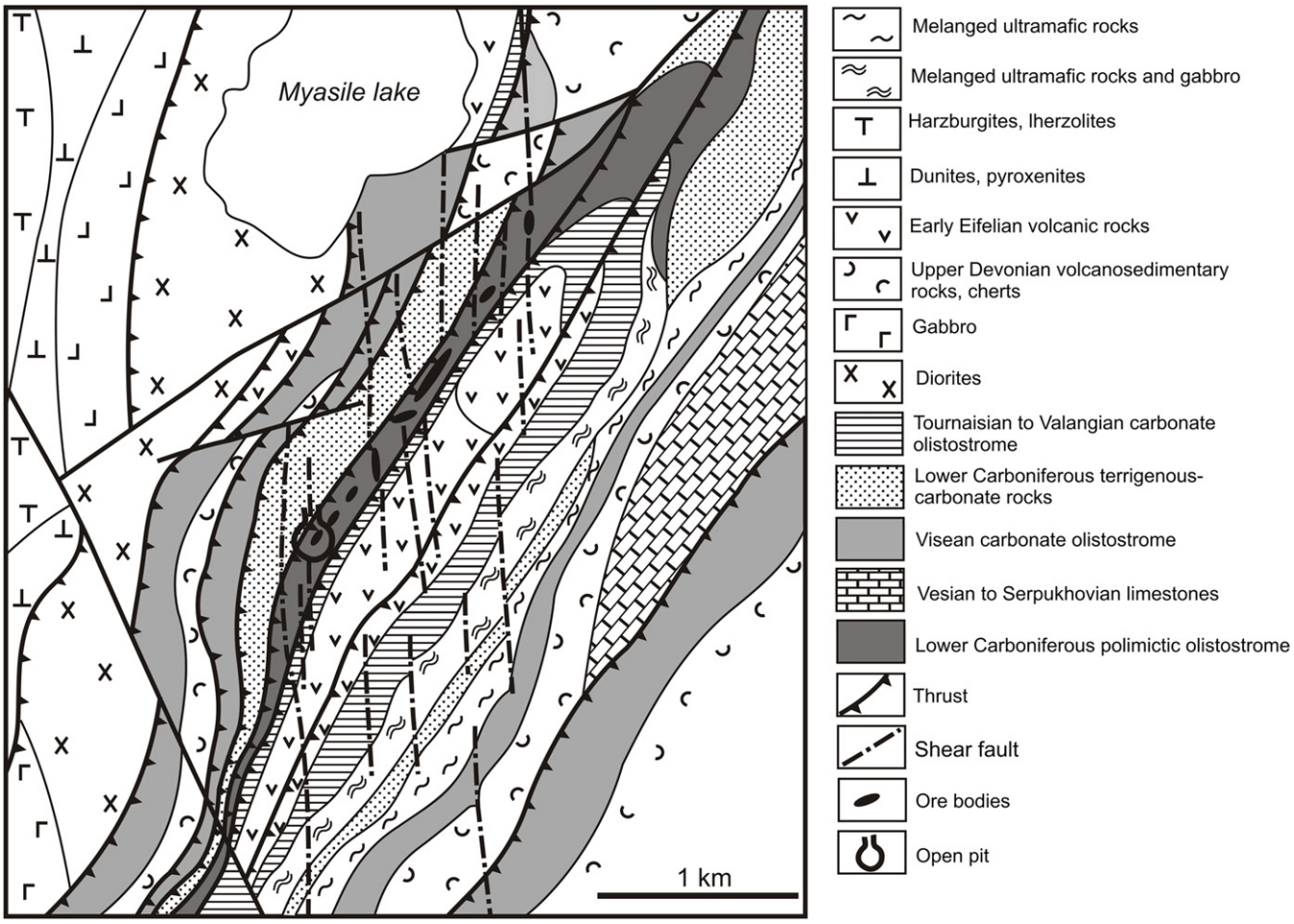

Fig. 13. Geological structure of the Mindyak deposit, simplified after Znamensky and Michurin (2013).

from −5.2 to −25.1‰. The $\delta^{34}S$ values of crystal pyrite from the ores of the Mindyak deposit range from −0.1 to −2.9‰ and are similar to those of pyrite from the Ganeevskoe deposit (−0.9 to +3.2‰).

6. Discussion

6.1. Geological features

The lode gold deposits reviewed in this contribution are thought to be formed during the late subduction and early collision stage of the Urals fold belt evolution (cf., Puchkov, 2016). The formation of supracrustal anatectic gabbro–tonalite–granodiorite–granite complexes is related to the early collision (Fershtater et al., 2010). These complexes are thought to be the source of magmatic fluids and metals for the lode gold deposits located in the Main Plutonic Axis of the Urals. High-grade metamorphism can result in total redistribution of small VHMS ore bodies (Vikent'ev et al., this issue), and scavenging of metals by fluid migrating along fault structures. These collision-related metamorphic fluids can react with sedimentary sulfides, which results in redistribution of metals dispersed in the volcanic and volcanosedimentary rocks. The evidence of remobilization and redeposition of metals is recorded in many VHMS deposits (Vikentyev, 2004), and they are apparently manifested along the entire Urals fold belt. The new ore minerals may precipitate due to decompression in fractures, cracks and detachments.

The studied gold deposits are located in the shear/fault zones (MUF zone) and are locally confined to the subsidiary faults (e.g., Ganeevskoe deposit within large Karagayly fault zone) (Znamensky, 2009; Znamensky and Michurin, 2013; Znamensky et al., 2014). Such structures (Zoheir and Lehmann, 2011; Kuzhuget et al., 2015; Qiu and Zhu, 2015) are favorable for accumulation of gold in fold belts (Groves et al., 1998, 2003; Dube and Gosselin, 2007), including listvenite-related deposits in ophiolitic zones.

Mafic volcanosedimentary rocks and serpentinites are the main host rocks at the studied deposits. The products of granitic magmatism are either absent (Ganeevskoe deposit) or occur as relatively thin dikes of plagiogranites (Mechnikovskoe deposit), microdiorites (Altyn-Tash) or diorites (Tyelga). Typically, these small intrusions are concordant with the orientation of the major structures of the deposits and are strongly altered (carbonatized, sericitized and pyritized), similarly to the host rocks, i.e., these bodies cannot be considered the source of metals and fluids. At the Ganeevskoe deposit, slightly altered gabbro and gabbrodiorite bodies are present (Znamensky and Michurin, 2013).

New mineral assemblages including carbonates (magnesite, minerals of the ankerite–dolomite series), quartz, mica, pyrite and albite were formed during alteration. Listvenites are formed after ultramafic rocks and their bright green color is a result of the Cr-bearing mica (fuchsite) formation. The influence of similar CO_2-bearing fluids on mafic rocks (basalts) produces beresites, which are mostly composed of the quartz ± albite–carbonate assemblage with sericite. The SiO_2 content in gold-bearing beresites of the Ganeevskoe deposit is 41.2–46.9 wt% and can reach 57 wt% in beresites from other deposits of the MUF. This is evidence that the studied beresites were formed after basalts or volcanoclastic rocks of basaltic composition, rather than after felsic rocks, which were accepted as the primary rocks for the classic beresites from Beresovskoe deposit (Sazonov, 1998). The alteration of primary rocks is related to the significant gain of CO_2, Na and

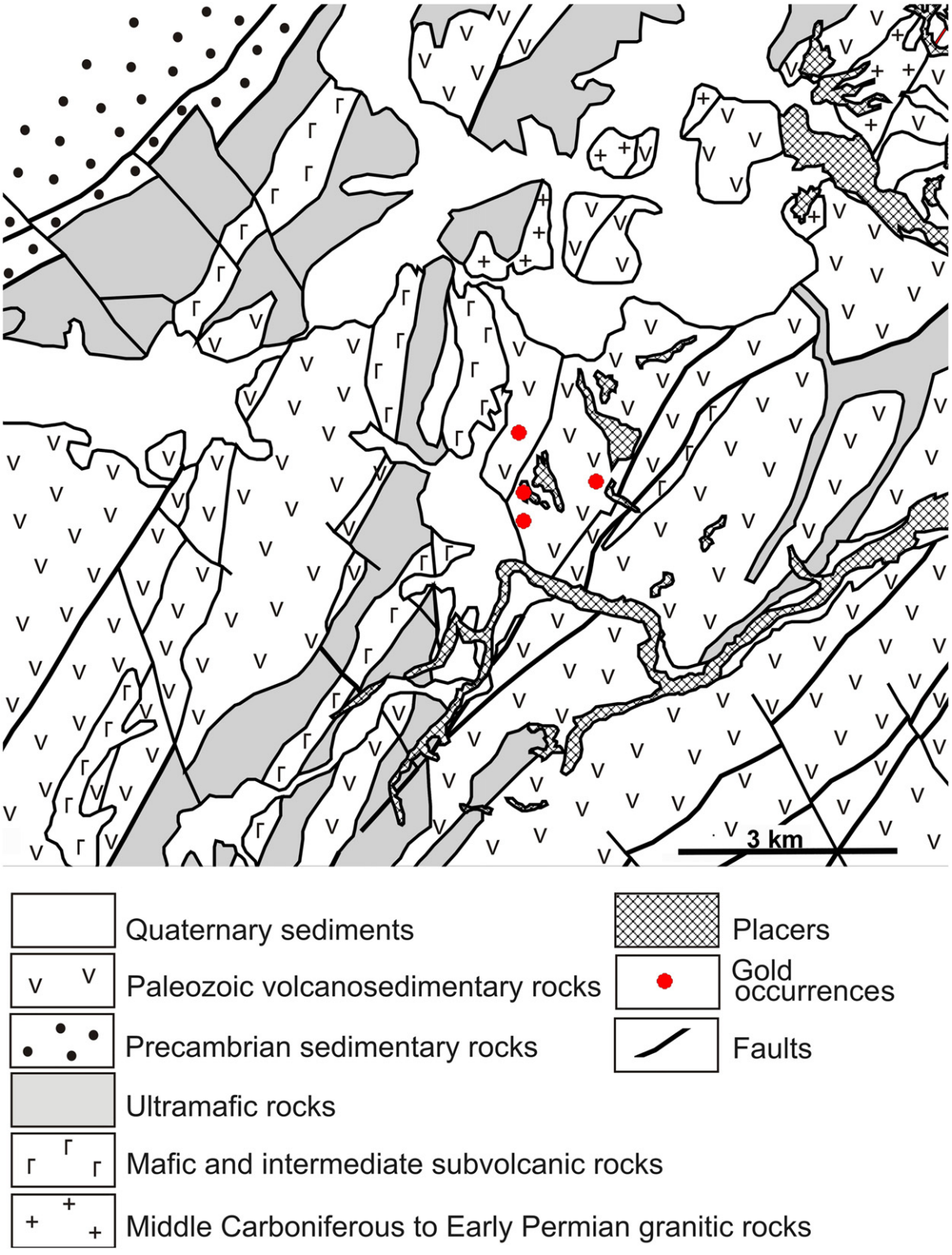

Fig. 14. Geological structure of the Karan–Alexandrovsky area, simplified after unpublished report of Galiullin (2007).

K (in the course of listvenitization), redistribution of Mg between ultramafic and mafic rocks, loss of Si and its deposition in thick quartz veins in extension zones. All these deposits contain disseminated pyrite and gold-bearing quartz veins, which were formed during the same stage of alteration of primary rocks. Thus, the studied deposits exhibit clear structural control of mineralization and mostly mica ± albite–quartz–carbonate style of ore-bearing metasomatites. The formation of quartz veins in metasomatites reflects the precipitation of excess silica, which was released from dark-colored minerals of ultramafic and mafic rocks under influence of CO_2-rich fluids.

Table 5
Oxygen isotopic composition ($\delta^{18}O_{VSMOW}$) in quartz, albite and equilibrium fluid ($\delta^{18}O_{H2O}$).

Sample number	Mineral	Location of sample	$\delta^{18}O_{VSMOW}$, ‰	$\delta^{18}O_{H2O}$, ‰
Mechnikovskoe deposit				
Len-72	Quartz	Veinlet in listvenite	15.4	6.4
Len-82			15.3	6.3
Len-85			15.3	6.3
Len-95			14.7	5.7
Len-97			15.3	6.3
Altyn-Tash deposit				
ar-4	Quartz	Vein in listvenite	13.6	4.6
ar-5			13.2	4.2
ar-6			13.3	4.3
ar-14			13.2	4.2
ar-27			13.4	4.4
ar-28			13.6	4.6
Ganeevskoe deposit				
3156-19a	Quartz	Veinlet in beresite	12.7	6.7
3156-19a(2)	Albite	Rock-forming mineral in beresite	10.1	–
3156-10	Quartz	Veinlet in listvenite	12.7	6.7
3156-10(2)		Rock-forming mineral in listvenite	12.6	6.6
3155-8		Quartz vein with galena and tellurides	12.0	6.0

Note: The quartz-water fractionation equation of Clayton et al. (1972) was used to calculate $\delta^{18}O_{H2O}$ for 250 °C for the Mechnikovskoe and Altyn-Tash, and 328 °C for Ganeevskoe deposits, respectively, that corresponds to the average trapping temperatures for both deposits.

6.2. Mineral composition

The predominance of pyrite and relatively high fineness of gold at the studied listvenite-related deposits are similar to those from typical orogenic gold deposits, including deposits localized in weakly metamorphosed metavolcanic and metavolcanoclastic rocks of greenstone belts (Dube and Gosselin, 2007). Some listvenite-related gold deposits contain arsenopyrite (Zoheir and Lehmann, 2011) or As-rich pyrite (Qiu and Zhu, 2015) as a major ore mineral. In the studied deposits, arsenopyrite is rare or absent in contrast to large gold deposits directly related to the granitic intrusives (e.g., Kochkar and Berezovskoe deposits), which are characterized by more diverse mineral composition with abundant As minerals such as arsenopyrite and fahlores (Sazonov et al., 1999; Bortnikov et al., 1999; Bortnikov, 2006). These deposits also contain relatively high-temperature chalcopyrite–pyrrhotite assemblage with native bismuth and Bi tellurides, as well as molybdenite and scheelite. Among the studied deposits, native Bi and Bi tellurides were identified only in the Altyn-Tash and Tyelga deposits, which are situated in the most foliated zone of the northern closure of the MZ (Table 6).

Galena, sphalerite, Ag- and Au tellurides, sulfosalts and low-fineness gold form late low-temperature mineral assemblages at the MUF and MZ deposits, as well as other listvenite-related lode gold deposits (Zoheir and Lehmann, 2011; Qiu and Zhu, 2015; Kuzhuget et al., 2015) and large gold deposits of the Urals (Sazonov et al., 1999, 2001; Ogorodnikov et al., 2004).

Table 6
Ore minerals of the deposits relating with listvenites.

Deposits	Major and minor	Rare
Tyelga (Sazonov et al., 1999)	**Pyrite**, chalcopyrite	Galena, fahlore, gold, tellurides of Bi, Ag, Au
Mechnikovskoe	**Pyrite**, chalcopyrite	Ag-tetrahedrite, cubanite, galena, gold, melonite, nickeline, pyrrhotite, sphalerite, stutzite, tennantite, petzite
Altyn-Tash (Melekestseva et al., 2011 and reference therein)	**Pyrite**, chalcopyrite, *secondary copper sulfides*	Aikinite, altaite, arsenopyrite, bornite, fahlore, frohbergite, galena, gersdorffite, gold, hessite, linnaeite, magnetite, melonite, millerite, molybdenite, native tellurium, pentlandite, pyrrhotite, sphalerite, tellurobismuthite, tetradymite
Ganeevskoe	**Pyrite**, chalcopyrite, galena	Aikinite, tennantite, galena, gold, hessite, millerite, pyrrhotite, petzite, polydymite, sphalerite
Mindyak (Murzin et al., 2001 and reference therein)	**Pyrite,** chalcopyrite, pyrrhotite	Arsenopyrite, breithauptite, gersdorffite, gold, millerite, sphalerite, tetrahedrite, ullmannite
Alexandrovskoye	**Pyrite**	No data

Notes: Ore-forming minerals are typed in bold.

6.3. Formation conditions based on fluid inclusion data

The formation conditions at the studied deposits are similar in terms of Na–Cl–H_2O–CO_2 ± CH_4 composition of fluids and formation temperatures. Although Ganeevskoe deposit is characterized by the wider range of T_h (150–329 °C), the average value of ~240 °C is similar to that from other studied deposits (~200 and ~250 °C, Table 4), as well as the maximum range of values. At the Altyn-Tash deposit, gold-bearing quartz was formed from two immiscible fluids, which is supported by: (a) homogenization of vapor-rich and liquid-rich inclusions over the same ranges of temperatures to vapor and liquid phases, respectively; (b) different salinity of vapor- and liquid-rich FIs, and (c) negative salinity vs. homogenization temperature trend (cf., Pichavant et al., 1982; Ramboz et al., 1982; Hurai, 2010; Chen et al., 2012). The fluid density and salinity are slightly higher for the fluid inclusions in quartz from the Altyn-Tash and Mechnikovskoe deposits (Fig. 15). The lowest and highest pressures of ore formation are estimated for the Mechnikovskoe and Ganeevskoe deposits, respectively. The low pressure was also calculated for the MUF gold deposits on the basis of calcite–dolomite thermometer: 0.5–0.66 and 0.7 kbar for the Mindyak (Murzin et al., 2001) and Tyelga (Sazonov et al., 1999) deposits. In general, these estimations are lower and the range of values is narrower in comparison with large deposits: 1.3–2.4 kbar for the Barramia deposit (Zoheir and Lehmann, 2011) or 1.02–3.66 or 0. 5–2.6 kbar for the Svetlinskoe and Kochkar deposits, respectively (Bortnikov, 2006); the formation of latter is believed to be related to the suprasubduction gabbro–tonalite–granodiorite–granite magmatism (Fershtater et al., 2010; Fershtater, 2013). Thus, the *PT* conditions of ore formation of small listvenite-related gold deposits of the South

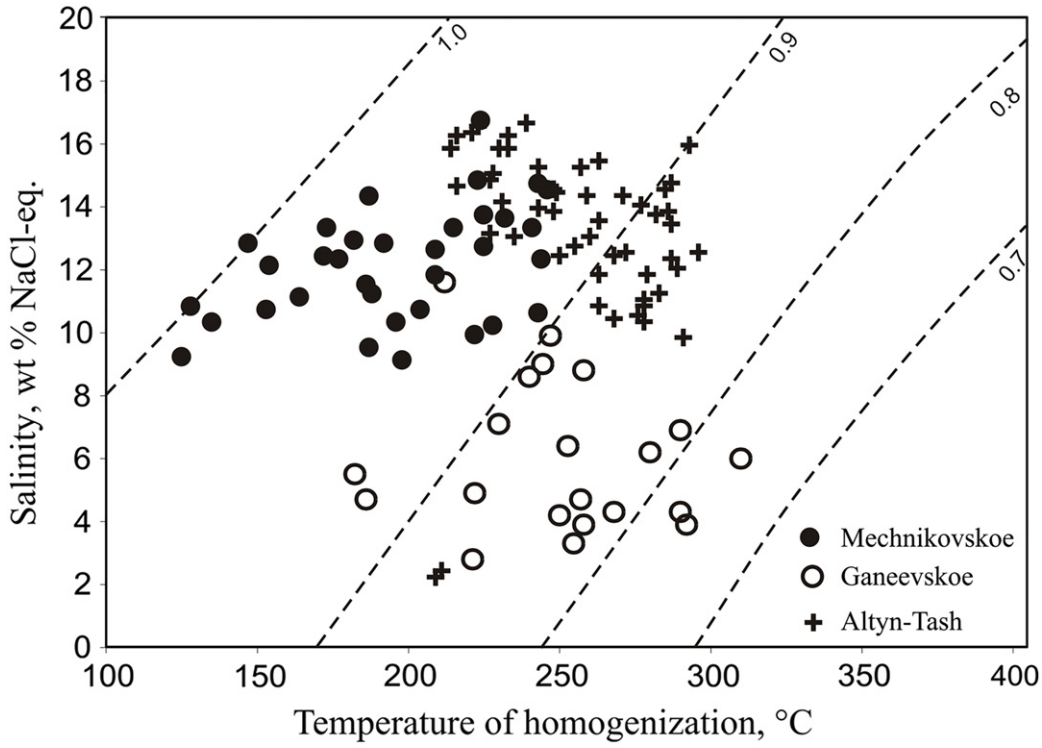

Fig. 15. Temperature vs. fluid salinity plot for fluid inclusions in quartz of the Mechnikovskoe, Altyn-Tash and Ganeevskoe deposits. Dash lines, density isolines of fluid according to (Wilkinson, 2001, Fig. 6).

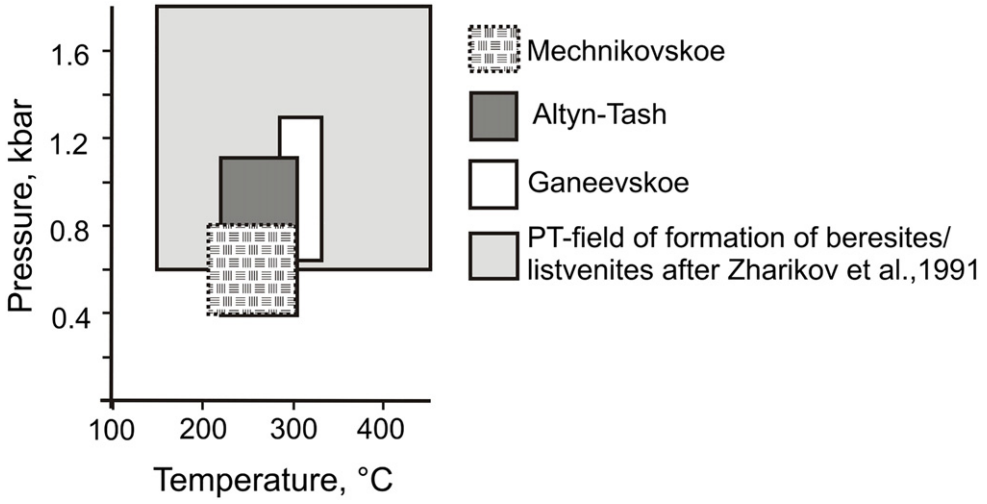

Fig. 16. PT-field of ore formation estimated using fluid inclusion data for studied deposits.

Urals are in agreement with those identified for listvenitization and beresitization processes and occupy a relatively low-pressure area (Fig. 16). This is consistent with the shear/fault geological setting of gold deposits, greenschists facies metamorphism of the host rocks and rare findings of arsenopyrite in the ores. Relatively low pressures at relatively high temperatures could be one more evidence of involvement of magmatic fluids in ore formation.

6.4. Source of fluids

Most data on isotopic composition of stable isotopes in minerals from the Urals gold deposits are known for large ore systems (e.g., Bortnikov et al., 1999; Bortnikov, 2006). The isotopic data on relatively small gold deposits of the MUF and MZ are scarce (Murzin et al., 2002; Znamensky and Michurin, 2013), thus the results of our studies are important for understanding of their origin.

The $\delta^{18}O_{H2O}$ values of the fluid in equilibrium with quartz were calculated at 250 °C (Mechnikovskoe and Altyn-Tash deposits) and 328 °C (Ganeevskoe deposit), which correspond to the average T_h. The $\delta^{18}O_{H2O}$ values in the fluid vary from 5.7 to 6.3‰ (av. 6.2‰, Mechnikovskoe deposit) and from 4.2 to 4.6‰ (av. 4.4‰, Altyn-Tash deposit) (Fig. 17). The calculated $\delta^{18}O_{H2O}$ values in the fluid from metasomatites and polymetallic vein of the Ganeevskoe deposit are 6.3–6.7 (av. 6.6‰) and 6.0‰, respectively (Fig. 17). A narrow range of $\delta^{18}O$ values in quartz

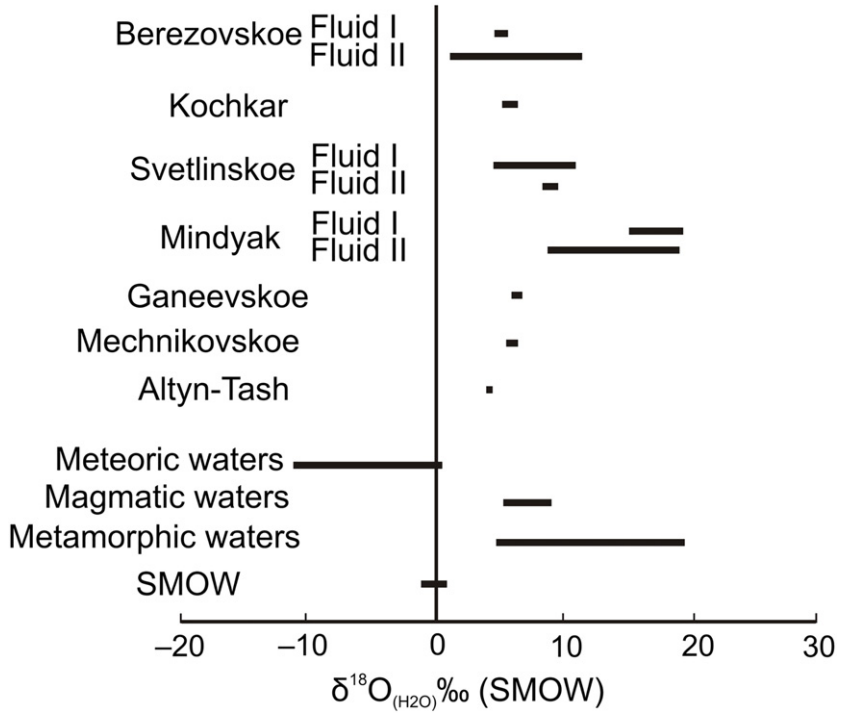

Fig. 17. Oxygen isotopic composition of equilibrium fluid for the Mechnikovskoe, Ganeevskoe and Altyn-Tash deposits in comparison with data on large orogenic gold deposits of the Urals after Bortnikov (2006). Oxygen isotopic composition of meteoric, magmatic and metamorphic waters is given after Sheppard (1986).

indicates homogeneous source of the fluid and no isotopic exchange between the host rocks and fluids (Goldfarb and Groves, 2015). This is in contrast with the data on large orogenic lode gold deposits of the South Urals, which show significant variations in oxygen isotopic composition of quartz and equilibrium fluid that is related to intense host rock/fluid interaction and several fluid sources (e.g., magmatic, metamorphic, meteoric) (e.g., Bortnikov et al., 1999; Bortnikov, 2006).

For the Mindyak deposit, the $\delta^{13}C_{CO2}$ and $\delta^{18}O_{H2O}$ values of the fluid in equilibrium with carbonates were calculated by Murzin et al. (2002) using the fractionation equations for the dolomite–CO_2 and calcite–CO_2 systems (cf., Golyshev et al., 1981; Ohmoto and Rye, 1979), taking into account the temperatures of mineral formation estimated from dolomite–calcite thermometer (Murzin et al., 2001, 2002). In the high-temperature fluid, the $\delta^{13}C_{CO2}$ and $\delta^{18}O_{H2O}$ values vary from −5.4 to +8.0 and from +15.7 to +25.7‰, respectively. The low-temperature fluid contains higher amounts of lighter carbon isotope ($\delta^{13}C_{CO2}$ = +1.6 to −22.4‰), whereas the $\delta^{18}O_{H2O}$ values show narrower range from +8.5 to +15.7‰. The carbon isotope composition of carbonates associated with disseminated ores corresponds to that of marine carbonates. In contrast to Mechnikovskoe, Altyn-Tash and Ganeevskoe deposits, the $\delta^{13}C_{CO2}$ and $\delta^{18}O_{H2O}$ values of the fluid of the Mindyak deposit indicate the isotopic exchange between the fluid and host rocks, and, particularly, black shales. A broad range of isotopic compositions may evidence the involvement of fluids from different sources. The heavier $\delta^{18}O_{H2O}$ values of the fluid are similar to those of metamorphic waters (Fig. 17).

Negative $\delta^{34}S$ values of nodular pyrite from the host black shales of the Mindyak deposit indicate sedimentary source of sulfur (Znamensky et al., 2014). The $\delta^{34}S$ values of crystal pyrite from the Mindyak and Ganeevskoe deposit are regarded as an evidence of the magmatic source of sulfur in the fluid (Znamensky and Michurin, 2013). These values fall into a range of variable sulfur isotopic composition of sulfides from the Urals VHMS deposits, which also show good evidences of magmatic contribution to their formation (Prokin and Buslaev, 1999). Thus, on the basis of available isotopic data, magmatic source of the fluid at the studied listvenite-associated gold deposits is most likely; involvement of some amount of water and carbon of host rocks to ore formation is recorded at the Mindyak deposit. Involvement of magmatic fluids in formation of listvenite-related gold deposits is consistent with the data on other gold deposits from ophiolitic belts (e.g., Zoheir and Lehmann, 2011).

6.5. Source of metals

It is accepted that the process of listvenitization is caused by the influence of late-orogenic granitic rocks, which produce Cl-rich carbon–aqueous fluids enriched in As, Sb and Hg (Sazonov et al., Zharikov et al., 2007). The presence of Cr, Ni, Co and Pt minerals in listvenites clearly indicates an ultramafic protolith (Likhoidov et al., 2007). For the South Urals deposits, the presence of Cr-bearing mica, Ni sulfides and sperrilite (the latter was found in small Borisovskie Zhily listvenite-related gold deposit within the Miass ore field; Artemyev, 2014) is an evidence for the involvement of serpentinites in their formation. The occurrence of abundant chalcopyrite in the ores of most reviewed deposits is in agreement with the elevated Cu content in the host mafic volcanic rocks of the Polyakovka, Irendyk and Karamalytash formations (120, 100 and 75 ppm, respectively), in contrasts to the felsic rocks of the Irendyk and Karamalytash formations (38 and 10 ppm, respectively) (Frolova and Burykova, 1977).

The source(s) of gold responsible for the formation of the listvenite-related gold deposits is debatable, as well as the source of precious metals in hydrothermal deposits in greenstone belts in general. It has been argued that ultramafic and mafic rocks in ophiolitic mélange could be a source of gold for the ophiolitic-hosted gold deposits of Eastern Desert of Egypt (Harraz, 2000), Sahlabad region (Aftabi and Zarrinkoub, 2013) and Sayi gold deposit, Xinjiang, NW China (Qiu and Zhu, 2015). Nevertheless, the Au grades in ores are about three orders of magnitude higher than those of their supposed source rocks

(5–11 ppb in ultramafic rocks, 15 ppb in volcanic rocks or 10 ppb in black shales, Boyle, 1979; Moss and Scott, 2001; Ketris and Yudovich, 2009). We believe that the formation of gold deposits with economic Au grades requires either reworking of very large rock volumes, or some additional mechanisms of extraction and accumulation of gold. The repeated removal of gold from rocks during multistage suprasubduction anatexis under high fluid saturation could be one of such mechanisms (Fershtater et al., 2010).

7. Concluding remarks

The listvenite-related lode gold deposits are located in large fault zones of the South Urals. They are relatively small but constitute the important sources for numerous gold placers in surrounding area. Economic Au grades at the Mechnikovskoe, Altyn-Tash and Ganeevskoe deposits are established in listvenites, beresites and accompanying quartz veins. Listvenites are developed after serpentinites and composed of quartz, fuchsite and carbonates (magnesite, dolomite) ± albite; beresites, which replace the volcanic and volcanoclastic rocks. These metasomatites consist of sericite, carbonates (dolomite, ankerite), quartz and albite. Pyrite and chalcopyrite are the major ore minerals associated with gold; pyrrhotite, Ni sulfides, galena, sphalerite and Au and Ag tellurides are subordinate and rare. Gold is mostly characterized by high fineness; the lower fineness is typical of gold in assemblage with polymetallic sulfides and tellurides.

The ores were formed from the $NaCl–CO_2–H_2O \pm CH_4$ fluids of moderate salinity and temperatures of 210–330 °C. The temperatures and oxygen isotopic composition of quartz, albite and equilibrium fluid in the gold-bearing rocks generally corresponds to those of typical orogenic deposits. Oxygen isotopic composition of quartz shows homogeneous source of the fluid and no fluid/host rock interaction during the ore formation. The calculated $\delta^{18}O$ values of H_2O in the fluid in equilibrium with quartz indicate that magmatic water is the most likely source of the fluid.

The source of metals remains ambiguous and we cannot rule out the extraction of metals from sulfides, which were deposited synchronously with volcanism of the island-arc stage of the South Urals evolution.

Conflict of interest

No conflict of interest.

Acknowledgements

The authors are grateful to the staff of the Bashkirian Gold Mining Company for support of the field work. We thank Dr. Olga Yu. Plotinskaya for permanent help and support, Dr. Valery V. Murzin, one anonymous reviewer, Handling Editor Svetlana G. Tessalina, and Chief Editor Franco Pirajno for their very detailed and constructive reviews, which helped us greatly to improve the paper. This work was supported by the State Contract of the Institute of Mineralogy UB RAS no. AAAA-A16-116021010244-O and the Urals Branch of the Russian Academy of Sciences, Russia (project no. 15-11-5-23).

References

Aftabi, A., Zarrinkoub, H., 2013. Petrogeochemistry of listvenite association in metaophiolites of Sahlabad region, eastern Iran: Implications for possible epigenetic Cu–Au ore exploration in metaophiolites. Lithos 156–159, 186–203.

Artemyev, D.A., 2014. Mineralogical and geochemical features of the Borisovskie Zhily gold deposit (Miass area, South Urals). In: Maslennikov, V.V., Melekestseva, I.Yu. (Eds.), Metallogeny of Ancient and Modern Oceans-2014. Miass, pp. 137–142 (in Russian).

Ash, C.N., Arksey, R.L., 1990. The listwanite-lode gold association in British Columbia. Geological Fieldwork 1989, British Columbia Geological Survey Branch. pp. 359–364.

Aydal, D., 1990. Gold-bearing listwaenites in the Araç Massif, Kastamonu, Turkey. Terra Nova 2, 43–52.

Baksheev, I.A., Kudryavtseva, O.E., 2004. Nickeloan tourmaline from the Berezovskoe gold deposit, Middle Urals, Russia. Can. Mineral. 42, 1065–1078.

Bodnar, R.J., Vityk, M.O., 1994. Interpretation of microthermometric data for H_2O-NaCl fluid inclusions. Fluid Inclusions in Minerals: Methods and Applications, pp. 117–130 Pontignana-Siena.

Borisenko, A.S., 1977. Study of salt composition of the fluid inclusions by cryometry. Geol. Geofiz. 8, 16–27 (in Russian).

Borodaevsky, N.I., 1948. Types of gold deposits associated with ultramafic rocks of the Miass and Uchaly regions of the South Urals. In: 200-Year Anniversary of Gold mining at the Urals. Proceeding of the UFAN, Sverdlovsk, pp. 316–330 (in Russian).

Borodaevsky, N.I., Borodaevskaya, M.B., 1946. Berezovskoe ore Field. p. 264 Moscow (in Russian).

Bortnikov, N.S., Sazonov, V.N., Vikent'eva, O.V., Vikent'ev, I.V., Murzin, V.V., Naumov, V.B., Nosik, L.P., 1998. Role of the magmatogenic fluid in the formation of the mesothermal Berezovsk gold–quartz deposit. Dokl Earth Sci. 363, 1078–1082.

Bortnikov, N.S., Stolyarov, M.I., Murzin, V.V., Prokof'ev, Yu.V., 1999. The Svetlinsk gold-telluride deposit, Urals, Russia: Mineral paragenesis, fluid inclusion and stable isotope studies. In: Stanley, C. (Ed.), Mineral Deposits: Processes to Processing. Proceedings of the Fifth Biennial SGA Meeting and the Tenth Quadrennial IAGOD Meeting. Balkema, Rotterdam, pp. 21–24.

Bortnikov, N.S., 2006. Geochemistry and origin of the ore-forming fluids in hydrothermal-magmatic systems in tectonically active zones. Geol. Ore Deposits 48, 1–22.

Botros, N.S., 2004. A new classification of the gold deposits of Egypt. Ore Geol. Rev. 25, 1–37.

Boyle, R.W., 1979. The geochemistry of gold and its deposits. Geol. Surv. Can. Bull. 280.

Buisson, G., Leblanc, M., 1986. Gold bearing listwaenites (carbonatized ultramaficrocks) in ophiolite complexes. In: Gallagher, M.J., Ixer, R.A., Neary, C.R., Prichard, H.M. (Eds.), Metallogeny of Basic and Ultrabasic Rocks. The Institution of Mining and Metallurgy, London, pp. 121–132.

Cathelineau, M., 1988. Cation site occupancy in chlorites and illites as a function of temperature. Clay Miner. 23, 471–485.

Chen, H., Chen, Y., Baker, M.J., 2012. Evolution of ore-forming fluids in the Sawayaerdun gold deposit in the Southwestern Chinese Tianshan metallogenic belt, Northwest China. J. Asian Earth Sci. 49, 131–144.

Clayton, R.N., O'Neil, J.R., Mayeda, T., 1972. Oxygen isotope exchange between quartz and water. J. Geophys. Res. 77, 3057–3067.

Dube, B., Gosselin, P., 2007. Greenstone-hosted quartz-carbonate vein deposits. Mineral Deposits of Canada: A Synthesis of Major Deposit-Types. District Metallogeny, the Evolution of Geological Provinces, and Exploration Methods. vol. 5. Geological Association of Canada, Mineral Deposits Division, pp. 49–73 Special Publication.

Fershtater, G.B., Krasnobaev, A.A., Borodina, N.S., Bea, F., Montero, P., 2007. Geodynamic settings and history of the paleozoic intrusive magmatism of the Central and Southern Urals: results of zircon dating. Geotectonics 41 (6), 465–486.

Fershtater, G.B., Kholodnov, V.V., Krasnobaev, A.A., Borodina, N.S., Zin'kova, E.A., Pribavkin, S.V., Kremenetsky, A.A., 2010. Au-bearing gabbro-tonalite-granodiorite-granite plutons of the urals: age, geochemistry, and magmatic and ore evolution. Geol. Ore Deposits 52 (1), 58–76.

Fershtater, G.B., 2013. Paleozoic Intrusive Magmatism of the Central and South Urals. p. 368 Yekaterinburg (in Russian with English conclusions).

Frolova, T.I., Burykova, I.A., 1977. Geosyncline Volcanism of the Urals. p. 279 Moscow, (in Russian).

Geological map of Russian Federation on a scale of 1: 1000000 (new series) N-40 (41) Ufa. In: Kozlov, V.I. (Ed.), 2001.

Goldfarb, R.J., Groves, D.I., 2015. Orogenic gold: common or evolving fluid and metal sources through time. Lithos 233, 2–26.

Golub, M.L., Berdnikov, P.G., Shaymardanova, R.M., 1982. New data on geochemistry of the Mindyak deposit. Problems of Mineralogy, Geochemistry and Genesis of Mineral Deposits of the South Urals, pp. 77–80 Ufa, (in Russian).

Golyshev, S.I., Padalko, N.L., Pechenkin, S.A., 1981. Fractionation of stable oxygen and carbon isotopes in carbonate systems. Geokhimiya 18, 85–99 (in Russian).

Groves, D.I., Goldfarb, R.J., Gebre-Mariam, M., Hagemann, S.G., Robert, F., 1998. Orogenic gold deposits: a proposed classification in the context of their crustal distribution and relationship to other gold deposit types. Ore Geol. Rev. 13, 7–27.

Groves, D., Goldfarb, R., Robert, F., Hart, C., 2003. Gold deposits in metamorphic belts: overview of current understanding, outstanding problems, future research, and exploration significance. Econ. Geol. 98, 1–29.

Halls, C., Zhao, R., 1995. Listvenite and related rocks: perspectives on terminology and mineralogy with reference to an occurrence at Cregganbaum, Co., Mayo, Republic of Ireland. Miner. Deposita 30, 303–313.

Hansen, L.D., Dipple, G.M., Gordon, T.M., Kellett, D.A., 2005. Carbonated serpentinite (listwanite) at Atlin, British Columbia: a geological analogue to carbon dioxide sequestration. Can. Mineral. 43, 225–239.

Harraz, H.Z., 2000. A genetic model for a mesothermal Au deposit: evidence from fluid inclusions and stable isotopic studies at El Sid Gold Mine, Eastern Desert, Egypt. J. Afr. Earth Sci. 30, 267–282.

Herrington, R., Zaykov, V., Maslennikov, V., Brown, D., Puchkov, V., 2005. Mineral deposits of the Urals and links to geodynamic evolution. Econ. Geol. 100th Anniversary Volume, 1069–1095.

Hurai, V., 2010. Fluid inclusion geobarometry: Pressure corrections for immiscible H_2O–CH_4 and H_2O–CO_2 fluids. Chem. Geol. 278, 201–211.

Kashkay, M.A., Allakhverdiev, Sh.I., 1965. Listvenites, Their Genesis and Classification. p. 143 Baku, (in Russian).

Ketris, M.P., Yudovich, Ya.E., 2009. Estimations of clarkes for carbonaceous biolithes: world averages for trace element contents in black shales and coals. Int. J. Coal Geol. 78 (2), 135–148.

Kisters, A.F.M., Meyer, F.M., Seravkin, I.B., Znamensky, S.E., Kosarev, A.M., Ertl, R.G.W., 1999. The geological setting of lode-gold deposits in the central southern Urals: a review. Geol. Rundsch. 87, 603–616.

Kolb, J., Ertl, R.G.W., Kisters, A.F.M., Meyer, F.M., 2000. Late-Permian orogenic gold mineralization at Kochkar, Urals. A GEODE – GeoFrance 3D Workshop on Orogenic Gold Deposits in Europe with Emphasis on the Variscides (ext. abstracts). BRGM, pp. 108–109.

Kuzhuget, R.V., Zaikov, V.V., Lebedev, V.I., Mongush, A.A., 2015. Gold mineralization of the Khaak-Sair gold-quartz ore occurrence in listwanites (western Tuva). Russ. Geol. Geophys. 56, 1332–1348.

Likhoidov, G.G., Plyusnina, L.P., Shcheka, Zh.A., 2007. The behavior of gold during listvenitization: experimental and theoretical simulation. Dokl. Earth Sci. 415, 723–726.

Melekestseva, I.Yu, Kotlyarov, V.A., Zaykov, V.V., Yuminov, A.M., 2011. Gold and silver minerals from Mechnikovskoe and Altyn-Tash deposits associated with listvenite, South Urals. In: Proceeding of All-Russian Conference Mineralogy of the Urals. Miass-Yekaterinburg, pp. 111–115 (in Russian).

Moss, R., Scott, S.D., 2001. Gold content of Eastern Manus basin volcanic rocks: implications for enrichment in associated hydrothermal precipitates. Econ. Geol. 96, 91–107.

Murzin, V.V., Bortnikov, N.S., Sazonov, V.N., 2002. Evolution of carbon and oxygen isotopic composition of carbonates and ore-forming fluid of the Mindyak gold deposits. In: Annual Proceedings of the Institute of Geology and Geochemistry UB RAS, Yekaterinburg, pp. 252–254 (in Russian).

Murzin V.V., Krinov D.I., Bortnikov N.S., Sazonov V.N., 2001. Stages, PTX formation conditions of ores and mode of occurrence of gold in ores from the Mindyak deposit, South Urals. In: Annual Proceedings of the Institute of Geology and Geochemistry UB RAS, Yekaterinburg, pp. 166–171 (in Russian).

Murzin V.V., Sazonov, V.N., Bortnikov, N.S., Krinov D.I., 2007. The origin of the Mindyak gold deposit, South Urals. Geology of the Urals and adjacent territories. In: Proceedings of Scientific Papers, Yekaterinburg, pp. 400–405 (in Russian).

Murzin, V.V., Shanina, S.N., 2007. Fluid regime and origin of gold-bearing rodingites from the Karabash alpine-type ultrabasic massif, Southern Ural. Geochem. Int. 45 (10), 998–1011.

Obolensky, A.A., Borisenko, A.S., 1978. Relation of listvenitization and ore formation at the mercury deposits of magnesium-carbonate-cinnabar (listvenite) type. Geology and Genesis of the Siberian Rare Metal and Polymetallic Deposits, pp. 27–42 Novosibirsk, (in Russian).

Ohmoto, H., Rye, R.O., 1979. Isotope of sulfur and carbon. In: Barnes, H.L. (Ed.), Geochemistry of Hydrothermal Deposits. John Wiley and Sons, pp. 509–567.

Ogorodnikov, V.N., Sazonov, V.N., Polenov, Yu.A., 2004. Minerageny of Shear Zones of the Urals. Part 1. Kochkar Ore Area. p. 216 Yekaterinburg, (in Russian).

Pichavant, M., Ramboz, C., Weisbrod, A., 1982. Fluid immiscibility in natural processes: use and misuse of fluid inclusion data. I. Phase equilibria analysis – a theoretical and geometrical approach. Chem. Geol. 37, 1–27.

Plotinskaya, O.Yu., Groznova, E.O., Kovalenker, V.A., Novoselov, K.A., Seltmann, R., 2009. Mineralogy and formation conditions of ores in the Bereznyakovskoe ore field, the Southern Urals, Russia. Geol. Ore Deposits 51, 371–397.

Plotinskaya, O.Yu., Grabezhev, A.I., Tessalina, S., Seltmann, R., Groznova, E.O., Abramov, S.S., 2017. Porphyry deposits of the Urals: geological framework and metallogeny. Ore Geol. Rev. 85, 153–173.

Prokin, V.A., Buslaev, F.P., 1999. Massive copper-zinc sulphide deposits in the Urals. Ore Geol. Rev. 14, 1–69.

Puchkov, V.N., 1997. Structure and geodynamics of the Uralian orogen. Geol. Soc. Spec. Publ. 121, 201–236.

Puchkov, V.N., 2017. General features relating to the occurrence of mineral deposits in the Urals: what, where, when and why. Ore Geol. Rev. 85, 4–29.

Qiu, T., Zhu, Y., 2015. Geology and geochemistry of listwaenite-related gold mineralization in the Sayi gold deposit, Xinjiang, NW China. Ore Geol. Rev. 70, 61–79.

Ramboz, C., Pichavant, M., Weisbrod, A., 1982. Fluid immiscibility in natural processes: use and misuse of fluid inclusion data. II. Interpretation of fluid inclusion data in terms of immiscibility. Chem. Geol. 37, 29–48.

Roedder, E., 1984. Fluid inclusions. Reviews in Mineralogy vol. 12. Mineralogical Society of America.

Rose, G., 1837. Mineralogisch-geognostische Reise nach dem Ural, dem Altai and dem Kaspischen Meere. Volume 1: Reise nach dem nördlichen Ural and dem Altai. C.V. Eichhoff Verlag der Sanderschen Buchhandlung, Berlin xxx plus 641 p. and plates I–VII.

Sazonov, V.N., 1984. Beresite–litvenite complex and accompanying mineralization: example of the Urals. p. 208 Sverdlovsk, (in Russian).

Sazonov, V.N., 1998. Gold-Bearing Metasomatic Associations in Fold Belts. p. 181 Yekaterinburg, (in Russian).

Sazonov, V.N., van Herk, A.H., de Boorder, H., 2001. Spatial and temporal distribution of gold deposits in the Urals. Econ. Geol. 96, 670–685.

Sazonov, V.N., Ogorodnikov, V.N., Koroteev, V.A., Polenov, Yu.A., 1999. Gold Deposits of the Urals. p. 570 Yekaterinburg, (in Russian).

Servakin, I.B., Pirozhok, P.I., Sjuratov, V.N., Khmelev, A.P., Znamensky, S.E., Kovalevsky, N.I., Pshenichny, G.N., Samusenko, A.K., Khamidullina, F.G., Grigor'ev, Yu.P., Kalinin, E.P., Chadchenko, A.V., 1994. Mineral resources of the Uchaly mining and processing enterprise. Ufa, 328p. (in Russian).

Sheppard, S.M.F., 1986. Characterization and isotopic variations in natural waters. Stable Isotopes in High Temperature Geological Processes. Rev. Mineral. vol. 16, pp. 165–183.

Simonov, V.A., 1981. Conditions of Mineral Formation of Non-Granitic Pegmatites. , p. 168 Novosibirsk, (in Russian).

Spiridonov, E.M., Pletnev, P.A., 2002. Zolotaya Gora deposit of cupriferous gold. p. 219 Moscow, (in Russian).

Spiridonov, E.M., Pletnev, P.A., Perelygina, E.V., Rapoport, M.S., 1997. Geology and Mineralogy of the Zolotaya Gora Deposit of Cuppreousn Gold (Karabash). MSU Publishing House, Middle Urals, Moscow, p. 197 (in Russian).

Valley, J.W., Kitchen, N., Kohn, M., Niendorf, C.R., Spicuzza, M.J., 1995. UWG-2, a garnet standard for oxygen isotope ratios: Strategies for high precision and accuracy with laser heating. Geochim. Cosmochim. Acta 59, 5223–5231.

Vikentyev, I.V., 2004. Formation and Metamorphism of Volcanic-Hosted Massive Sulfide Deposits. p. 344 Moscow (in Russian).

Wilkinson, J.J., 2001. Fluid inclusions in hydrothermal ore deposits. Lithos 55, 229–272.

Yaghubpur, A., Abedi A., 2005. Preliminary investigation on the economic mineralization in listwaenites from Sahl-Abad Area, Southeast Birjand, Iran. Goldschmidt Conf. Abst., A1048.

Yigit, O., 2006. Gold in Turkey – a missing link in Tethyan metallogeny. Ore Geol. Rev. 28, 147–179.

Zaykov, V.V., Tairov, A.D., Zaykova, E.V., Kotlyarov, V.A., Yablonsky, L.T., 2012. Precious metals in ores and ancient gold jewelry of the South Urals. Yekaterinburg, 232p. (in Russian).

Zharikov, V.A., Pertsev, N.N., Rusinov, V.L., Callegari, E., Fettes, D.J., 2007. Metasomatism and metasomatic rocks. <https://www.bgs.ac.uk/scmr/docs/papers/paper_9.pdf>.

Zharikov, V.A., Zaraisky, G.P., 1991. Experimental modeling of wall-rock metasomatism. In: Korzhinskii, D.S., Perchuk, L.L. (Eds.), Progress in Metamorphic and Magmatic Petrology: A Memorial Volume in Honour. Cambridge Univ. Press, NY, pp. 197–246.

Znamensky, S.E., 2009. Structural Condition of Formation of Gold Deposits at the Eastern Slope of the South Urals. p. 345 Ufa, (in Russian).

Znamensky, S.E., Michurin, S.V., 2013. Formation conditions of the Mindyak gold–sulfide deposit (Southern Ural): structural and isotopic-geochemical issues. Litosfera 4, 121–135 (in Russian with English abstract).

Znamensky, S.E., Michurin, S.V., Velivetskaya, T.A., Znamenskaya, N.M., 2014. Structural conditions of formation and matter sources of the Ganeevskoe gold deposit (Southern Ural). Litosfera 6, 118–131 (in Russian with English abstract).

Zoheir, B., Lehmann, B., 2011. Listvenite-lode association at the Barramiya gold mine, Eastern Desert, Egypt. Ore Geol. Rev. 39, 101–115.